



저작자표시-비영리-변경금지 2.0 대한민국

이용자는 아래의 조건을 따르는 경우에 한하여 자유롭게

- 이 저작물을 복제, 배포, 전송, 전시, 공연 및 방송할 수 있습니다.

다음과 같은 조건을 따라야 합니다:



저작자표시. 귀하는 원저작자를 표시하여야 합니다.



비영리. 귀하는 이 저작물을 영리 목적으로 이용할 수 없습니다.



변경금지. 귀하는 이 저작물을 개작, 변형 또는 가공할 수 없습니다.

- 귀하는, 이 저작물의 재이용이나 배포의 경우, 이 저작물에 적용된 이용허락조건을 명확하게 나타내어야 합니다.
- 저작권자로부터 별도의 허가를 받으면 이러한 조건들은 적용되지 않습니다.

저작권법에 따른 이용자의 권리는 위의 내용에 의하여 영향을 받지 않습니다.

이것은 [이용허락규약\(Legal Code\)](#)을 이해하기 쉽게 요약한 것입니다.

[Disclaimer](#)

공학석사 학위논문

영상기술 기반 축계 토크 측정 연구

A Study on Torque Measurements of Rotating Shafts
with Imaging Technique



지도교수 도덕희

2018년 2월

한국해양대학교 대학원

냉동공조공학과

김영환

본 논문을 김영환의 공학석사 학위논문으로 인준함



위원장 : 김동혁 (인)

위원 : 김성춘 (인)

위원 : 도덕희 (인)

2017 년 12 월 19 일

한국해양대학교 일반대학원

Content

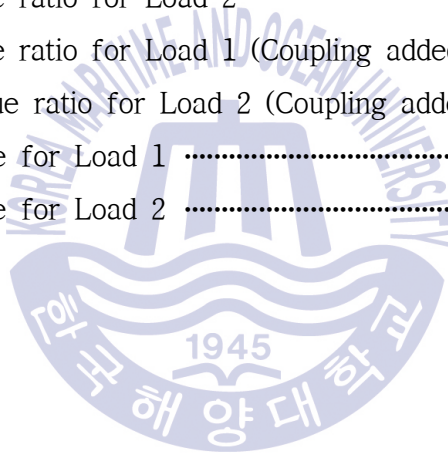
List of Tables	iv
List of Figures	v
Abstract	vii
1. Introduction	1
1.1 Background	1
1.2 Objectives	2
2. Power and Torque Variable Formulation	3
2.1 Power Variable	3
2.2 Torque Variable	5
2.2.1 Torque Variable Formulation	5
2.2.2 Shaft Torque Variable Formulation	6
3. Principle of Imaging Technique for Torque Measurements	11
3.1 Conventional Torque Measurement Systems	11
3.2 Non-Contact Image Technique Based Torque Measurement	15
3.2.1 Experimental Setup	15
3.2.2 Experimental Procedure	20
3.2.3 Image Technique Algorithm	21

3.3 Experimental Results and Discussions	24
3.3.1 Torque Transducer Measurement Results	24
3.3.2 PIV Based Torque Measurement Results	26
3.3.3 Measurement Results Comparison	39
3.3.4 Relevance of Coupling Stiffness	41
3.3.5 Revised Torsional Stiffness	42
3.3.6 Power Results	44
 4. Conclusions	 46
 Reference	 47
 감사의 글	 48



List of Tables

Table 1 Torque with respect to RPM, Load 1	24
Table 2 Torque with respect to RPM, Load 2	24
Table 3 Torsion Angle with respect to RPM, Load 1	31
Table 4 Torsion Angle with respect to RPM, Load 2	35
Table 5 Torsion Angle with respect to RPM, Load 1 and Load 2	36
Table 6 Torque with respect to RPM	37
Table 7 Torque value ratio for Load 1	39
Table 8 Torque value ratio for Load 2	39
Table 9 Torque value ratio for Load 1 (Coupling added)	43
Table 10 Torque value ratio for Load 2 (Coupling added)	43
Table 11 Power value for Load 1	44
Table 12 Power value for Load 2	44



List of Figures

Fig. 1 Torsional Angle Diagram	6
Fig. 2 Ring with radius R	8
Fig. 3 Piano Tape	12
Fig. 4 Tacho-Meter Signal illustration	12
Fig. 5 Pulse difference in shaft rotation	13
Fig. 6 Experimental Layout	16
Fig. 7 Random Pattern (Left Image, Right Image)	17
Fig. 8 Exposure time 0.000015s (Left 200 RPM, Right 1000RPM)	18
Fig. 9 Exposure time 0.000001s (Left 200 RPM, Right 1000RPM)	18
Fig. 10 Curve fitting error for common peak-fit functions	23
Fig. 11 Torque results from Torque Transducer for Load 1	25
Fig. 12 Torque results from Torque Transducer for Load 2	25
Fig. 13 Angle Change for 200 RPM with Load 2	26
Fig. 14 Angle Change for 800 RPM with Load 2	26
Fig. 15 Angle Change for 800 RPM with Load 2, Zoomed at peak	27
Fig. 16 Torsion Angle for 200 RPM with Load 1	28
Fig. 17 Torsion Angle for 300 RPM with Load 1	28
Fig. 18 Torsion Angle for 400 RPM with Load 1	29
Fig. 19 Torsion Angle for 500 RPM with Load 1	29
Fig. 20 Torsion Angle for 600 RPM with Load 1	30
Fig. 21 Torsion Angle for 700 RPM with Load 1	30
Fig. 22 Torsion Angle for 800 RPM with Load 1	31
Fig. 23 Torsion Angle for 200 RPM with Load 2	32
Fig. 24 Torsion Angle for 300 RPM with Load 2	32
Fig. 25 Torsion Angle for 400 RPM with Load 2	33
Fig. 26 Torsion Angle for 500 RPM with Load 2	33

Fig. 27 Torsion Angle for 600 RPM with Load 234

Fig. 28 Torsion Angle for 700 RPM with Load 234

Fig. 29 Torsion Angle for 800 RPM with Load 235

Fig. 30 Torque for Load 138

Fig. 31 Torque for Load 238

Fig. 32 Torque value comparison for Load 140

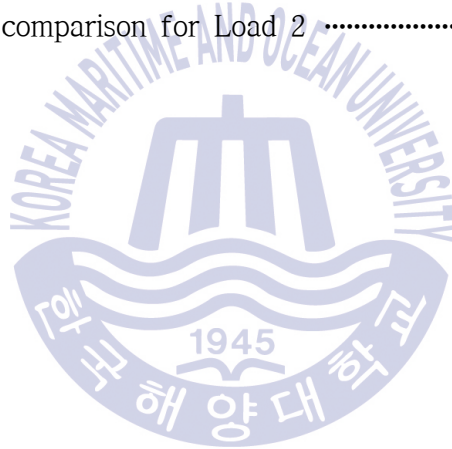
Fig. 33 Torque value comparison for Load 240

Fig. 34 Torque value comparison for Load 1 (Coupling added)42

Fig. 35 Torque value comparison for Load 2 (Coupling added)42

Fig. 36 Power value comparison for Load 145

Fig. 37 Power value comparison for Load 245



A study on Torque Measurements of Rotating Shafts with Imaging Technique

Kim, Yeong Hwan

Department of Refrigeration and Air-Conditioning Engineering
Graduate School of Korea Maritime and Ocean University

Abstract

Torque is a fundamental property of rotational force that is constantly reviewed throughout the process of modeling and inspecting mechanical engines. Engine manufacturers use torque data to calculate numerous engine qualities such as power consumption, efficiencies and failures. It is a core element that enables comparing modeled computational data to manufactured engine data. Recently, torque meter such as Kyma Shaft Power meter (KPM) is broadly used in ship industries. It has been a reliable source of measuring torque, yet it is very expensive and large in size. A relatively inexpensive and lighter torque sensing method that is not restricted to shaft diameter is in demand.

Many theories and methods for torque measurement have been proposed. One of them is to use Particle Image Velocimetry (PIV). Unlike conventional measurement methods for torque is to use contact type torque sensors, PIV is a non-contact method. The advantage of non-contact measurement method for torque is that it is not limited to diameter of the shaft.

Conventional torque sensors are not universally applicable for different size of shafts.

Torque of a shaft is related to torsional angle and torsional stiffness. When a shaft rotates, the load in the shaft twists the shaft and creates torsional angle variations. The magnitude of this angle is related to the diameter, the length, and the material of the shaft. Therefore, if the torsional angle and the material property of the shaft are given, the magnitude of the torque can be measured. PIV is able to verify the pattern of the image displacements by applying patterns on the shaft. This method allows us to effectively measure the torsional angle of a running shaft, and has the potential of becoming mainstream torque measurements. However, it is questionable if it is as reliable as contact type torque sensors. In this paper, the performances of a torque measurement system based on PIV and a contact type measurement system are compared. The torque results obtained by PIV method in this study reach up to 96% of the results obtained by contact type torque sensor.

KEY WORDS: Torque 토크; Torsional Angle 비틀림 각도; Particle Image Velocimetry 입자영상유속계; Torsional Stiffness 비틀림 강성; Visualization 가시화;

영상기술 기반 축계 토크 측정 연구

Kim, Yeong Hwan

Department of Refrigeration and Air-Conditioning Engineering
Graduate School of Korea Maritime and Ocean University

Abstract

토크(Torque)는 여러 공업 분야에서 다양하게 사용되는 기계적 표현법이다. 특히 석박 및 자동차 분야에서 토크란 엔진의 설계 및 검증 시 필수적으로 검토해야하는 변수중 하나이다. 엔진 설계 시 토크를 우선적으로 선정하여야 엔진의 성능 및 힘을 결정 할 수 있으며 제작된 엔진의 검증 또한 토크 측정으로부터 시작된다. 엔진으로부터 힘의 전달을 담당하는 축계의 안전성 검토 및 향상 또한 토크가 필요하다. 토크는 엔진 설계부터 검증까지 폭넓게 사용되기 때문에 토크는 여러 가지 방식으로 측정되어왔으며 이는 축의 비틀림 각 측정이 필수이다.

지금까지 여러 가지 토크 측정방식이 제기되어 왔으며 본 논문에서는 가시화를 활용한 토크 측정법에 대하여 설명하고 있다. 전통적인 신뢰성이 높은 토크 측정 방식은 접촉식이다. 가시화를 통한 토크 측정법은 카메라를 활용하기 때문에 비접촉식이며 여러 가지 크기의 축 직경에 사용 가능함으로 범용성이 접촉식보다 좋다.

축의 토크는 축이 회전함에 따라 발생하는 비틀림 각과 축의 물성치인 비틀림 강성에 연관성을 가진다. 따라서 비틀림 각과 비틀림 강성을 구한다면 축계 가해지는 토크를 살출할 수 있다. 가시적 토크 측정 방식은 입자영상

유속계를 활용하여 측에 설치된 랜덤 패턴을 인식하여 측의 여러 지점에서 측의 이동량을 확인할 수 있다. 하지만 가시화를 통한 토크 측정법은 새로운 측정법이기에 때문에 접촉식 토크 측정법에 비해 신뢰도 평가가 부족하다. 따라서 본 논문에서는 PIV를 활용한 가시적 토크 측정법과 접촉식 토크 측정법의 토크 측정 결과를 비교 분석한다. 가시적 토크 측정 결과는 접촉식에 비해 최대 96%의 동일성을 가지는 것을 확인했으며 이는 가시적 토크 측정법이 접촉식 토크 측정법을 대체할 수 있는 가능성을 확인하였다.

KEY WORDS: Torque 토크; Torsional Angle 비틀림 각도; Particle Image Velocimetry 입자영상유속계; Torsional Stiffness 비틀림 강성; Visualization 가시화;



1. Introduction

1.1 Background

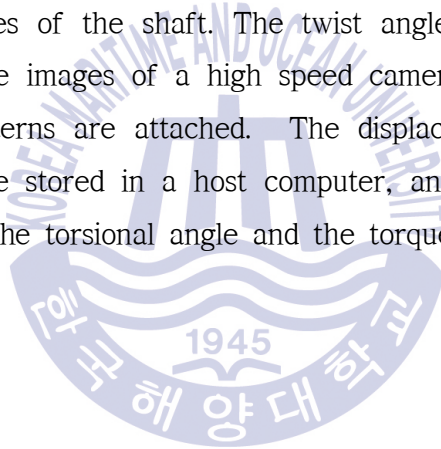
Torque is a fundamental mechanical expression that is used in various industries. Torque is a crucial variable in automotive and ship manufacturing, since it is used to verify engine designs and inspections. During engine design, torque must be considered in the initial stages for it is used to calculate power and performance of the engine. Also, torque is the first variable that is desired for inspecting safety of the already manufactured or delivered engines. Furthermore, torque is used to verify and inspect the safety of a shaft that delivers power from the engine. The variety of torque variable usage, from initial design to inspection of manufactured engines, led the industry to create demand for sensors and techniques that accurately measures torque. There are mainly two types of torque sensing, contact type (Kyma, 2010) and non-contact type sensors (Polytech, 2017). Contact type mechanical sensors use sensors such as slip ring, or strain gauges to measure the torque. Non-contact type sensors use lasers to measure torque.

Currently, most torque measurement is conducted through mechanical contact type sensors. The disadvantage of the contact type are that as engines get bigger sensors need to be bigger as well. This causes the sensor to become heavier and more expensive. Another disadvantage is that the sensor needs to be attached to the shaft.

This paper proposes to use imaging technique based on Particle Image Velocimetry(PIV) (Adrian, 1991) to measure torque that overcomes the limitations of contact type sensors.

1.2 Objectives

The objective of this paper is to introduce a new torque measurement method using imaging technique based on PIV. Unlike most conventional contact type torque measuring sensors, this technique uses high speed camera. Therefore, this paper proposes a non-contact torque measurement system in which the relation between the torsional angles and torque variation are made. A torque is a mechanical behaviour which is created when a twist of the shaft to the rotational direction occurs. Therefore, if the twist angle of the rotational shaft can be measured accurately, the torque can be measured with material properties of the shaft. The twist angles of the shaft can be quantified by using the images of a high speed camera of the rotating shaft on which random patterns are attached. The displacements calculated from the image patterns are stored in a host computer, and the accumulated data are used to calculate the torsional angle and the torque of the shaft.



2. Power and Torque Variable Formulation

2.1 Power Variable

Force is created when acceleration is applied to a mass of an object. Fundamental force calculations allow scientists and engineers to start designing structures, automobiles, and ship effectively and safely. Power is also an extending variable derived from force. Historically, power was not accurately quantified. Thus, in the old days power was calculated by the most popular means of transportation, horses. A horse that can draw a cart for one minute was set to be one horse power (hp). Nowadays, horse power is illustrated in W (Watt), or kW (Kilo Watt). In engines, power is mostly used to determine the performance of the manufactured engines. Since power and torque is closely related it is important to formulize power.

Force is acceleration applied to a mass of an object and the force equation is illustrated in equation (2.1)

$$\vec{F} = m\vec{a} \quad (2.1)$$

Here,

m : Mass of an object

\vec{a} : Acceleration applied to mass

Also, when this force is moved with a displacement of d , it is said that the object has worked. The unit of work is defined in Joule and the equation of work is shown in equation (2.2)

$$W = \vec{F} \cdot \vec{d} \quad (2.2)$$

Here,

\vec{d} : Displacement the mass moved

Now, power is work done in unit of time, and the unit for power is Watt. Equation (2.3) shows the power equation.

$$P = \frac{W}{t} \quad (2.3)$$

Here,

t : Time the mass moved

Therefore, according to equations (2.1) to (2.3), when mass, acceleration, force, displacement, and time is known power can be calculated. Another variable that is as important as power in engine is the torque variable.

2.2 Torque Variable

2.2.1 Torque Variable Formulation

When force can be regarded as mechanical property that pulls and pushes objects along a line, torque can be regarded as a mechanical property that rotates objects. For example, when a door is opened, the force that rotates the door to open is called torque. Mathematically, torque is derived by multiplying perpendicular force with distance from the fulcrum. Since torque is derived by multiplying force and displacement, the unit is illustrated in Nm. The torque equation is shown in equation (2.4).

$$\vec{\tau} = \vec{r} \times \vec{F} \quad (2.4)$$

Here,

\vec{r} : Displacement from the axis of rotation

However, the desired torque in this paper is torque in a rotating shaft, and shaft torque is in relation with the material property and torsional angle. Equation (2.4) neither has information about material property nor torsional angle. Thus, equation (2.4) is not sufficient to calculate shaft torque and further torque formulation is required.

2.2.2 Shaft Torque Variable Formulation

This paper is mainly about using visualization techniques to find the torque load acting on the rotating shaft. When the torque load on the shaft is captured through visualizations, the visualized output data is formed into twisted angle displacements. Since the torque and the twisted angle of the shaft are closely related, it is important to derive a torque formula that has angle displacements.

Before deriving the torque formula it is important to figure out the physical meaning of the twist angle in the shaft system. When torque load is applied to a shaft, the shaft rotates with a twist angle between the center of the rotating shaft and the rotating shaft surface. Simple analogy of the twist angle is shown in Fig. 1.

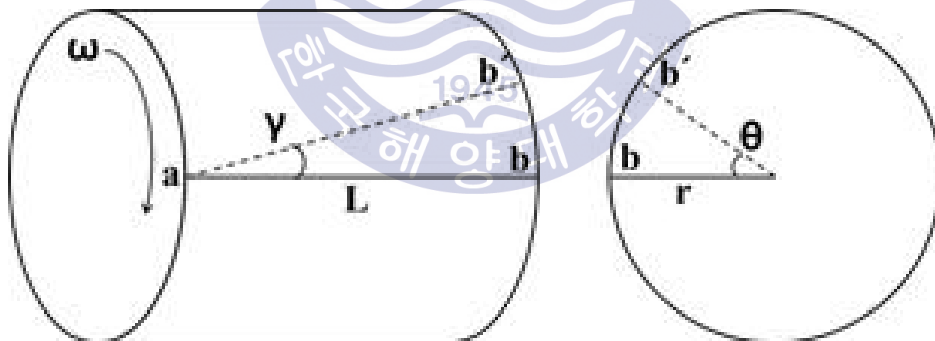


Fig. 1 Torsional Angle Diagram

When a shaft starts rotating, typical shaft would show behaviour shown in Fig. 1. When the shaft is remaining still and not rotating, the two points a and b at the ends of the shaft is parallel to each other. However, when the shaft starts rotating, Fig. 1 shows that point a moves ahead of the point b.

Therefore, due to twisting shaft point b becomes b' . The angle between b and b' is called the twist angle(θ) or torsional angle(θ).

The torsional angle can be derived by the following method. By setting the angle between lines ab and ab' to be γ , the arc bb' can be represented by the relationship between shaft length (L) and γ . Also, the arc length can be represented in relationship between radius(r) of the shaft and torsional angle(θ).

Using the ratio between shear strain and shear stress, the shear modulus can be calculated. The equation (2.5) shows the equation for shear modulus.

$$G = \frac{\tau}{\gamma} \tag{2.5}$$

Here,

G : Shear Modulus (MPa)

τ : Shear Stress (MPa)

Using the angle informations and equation (2.5), equation (2.6) can be derived which is equation for shear stress.

$$\tau = \frac{G\theta r}{L} \tag{2.6}$$

Fig. 2 is a figure of shear stress being applied to the radius of a typical ring.

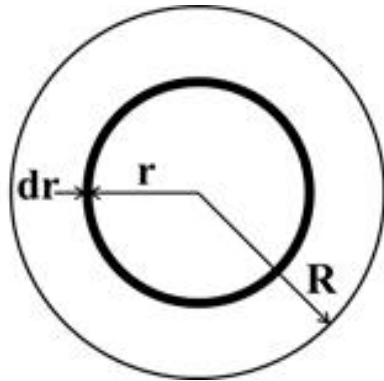


Fig. 2 Ring with radius R

The area of the ring can be calculated by using the equation (2.7).

$$dA = 2\pi r dr \quad (2.7)$$

Using equations (2.6) and (2.7) the shear force can be derived.

Also, by multiplying length r to the shear force, one can derive the torque applied to the ring. The torque equation is shown in equation (2.8).

$$dT = \tau 2\pi r^2 dr \quad (2.8)$$

The torque calculation of the ring surface cross-section is shown in equation (2.9). Since the integration part of the equation (2.9) is 2nd moment of inertia one can replace it with J and rearrange equation (2.9) to equation (2.10).

$$T = \frac{G\theta}{L} 2\pi \int_0^R r^3 dr \quad (2.9)$$

$$T = \frac{G\theta}{L} J \quad (2.10)$$

Here,

T : Torque of the shaft (Nmm)

J : 2nd moment of inertia (mm⁴)

Using equation (2.10) shows the relationship between torsional angle and torque. Also, shear modulus in equation (2.10) can be related to the 2nd moment of inertia which is shown in equation (2.11).



$G = \frac{kL}{J}$ (2.11)

Here,

k : Torsional stiffness (Nmm/rad)

Finally, substituting equation (2.11) into equation (2.10) the following torque equation (2.12) can be derived.

$$T = k\theta \quad (2.12)$$

Equation (2.12) shows that torque can be calculated by only using two variables, torsional stiffness and shaft torsional angle. Generally, torsional

stiffness of a shaft can be known from the manufacturer of the shaft. This is because the stiffness of the shaft is dependent on the material of the shaft, and the stiffness of the shaft would change with respect to the material of choice by the manufacturer. Therefore, one can say that the torsional stiffness variable is a known value. However, torsional angle is a different story. Torsional angle can only be retrieved while operating the shaft system and is an unknown variable. This means if one can find the torsional angle from the operating shaft, one can also calculate the torque applied to the shaft.

Further inspecting the equations listed above, one can also calculate the power. Power of an engine is also a very important variable due to its versatile uses in safety inspections and design flaws. Power is relatively easy to calculate once torque is correctly calculated. Since power of an engine is related to the rotations and rotating time of the shaft, the power equation should have angular velocity variable in its equation. The equation (2.13) shows the relationship between torque and power.

$$P = \frac{2\pi\omega T}{60} \quad (2.13)$$

Here,

P : Power of source (W)

ω : Rotating speed of a shaft (RPM)

3. Principle of Imaging Technique for Torque Measurements

3.1 Conventional Torque Measurement Systems

Generally, torque measurement starts from installing steel ring on the shaft. Then the shaft power meter attached to the ring calculates the torque applied to the shaft while the shaft is operating. This kind of measuring system is categorized into contact type torque measurement sensor. Disadvantages of contact type torque sensors are that as shaft diameter becomes larger the sensor becomes larger as well. Also, since the size becomes larger the weight of the sensor also becomes heavier. Another disadvantage is that contact type torque sensors have limited diameter size. Since the sensor has to be on the shaft itself, a small diameter torque sensor cannot be applied to large diameter shaft, and large diameter torque sensor is not applicable to the small diameter shaft. This limitation causes torque sensor to be relatively inconvenient and not practical. Currently, most widely used contact type torque sensor in the ship industry is the Kyma Shaft Power Meter (Kyma, 2010).

Other than contact type torque sensors, there are also non-contact type torque sensors. Non-contact type sensors are typically made with application of laser or optical systems. One way of using optical sensors to measure torque is by using Tacho-meter. Two tacho-meters can be used in conjunction to find the torsional angle between two end points on the shaft. However, for tacho-meter to receive data signals the shaft should have a tape called piano tape attached. A piano tape is a special kind of reflective tape that allows the tacho-meter to receive signals from. The basic concept of a tacho-meter is to apply a small reflective tape on a rotating object to receive one signal for every one rotation. Since there is only one reflector the tacho-meter

would only read one signal per rotation allowing one to calculate RPM of a rotating object. A piano tape is a distinctive reflective tape that allows the tachometer to read signals in steps. For easier analogy Fig. 3 shows the shape of piano tape.

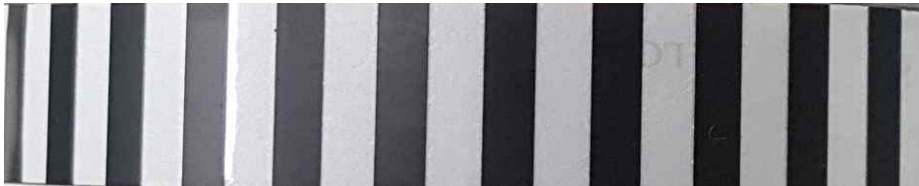


Fig. 3 Piano Tape

A piano tape consists of reflective parts (White) and unreflective parts (Black). Tachometer reads signal when the two white and black parts interchange. This way, one can determine how many pulses are read during one revolution. The pulse signal from the tachometer is illustrated in Fig. 4.

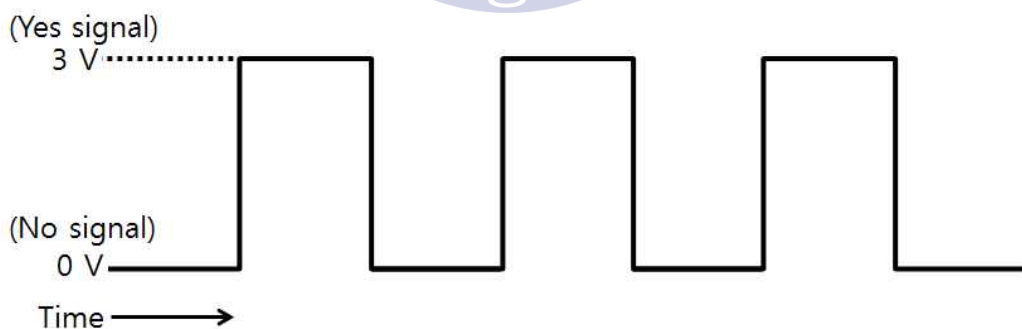


Fig. 4 Tacho-Meter Signal illustration

Using the method at the two endpoints of the shaft one can determine the pulse time difference to find shaft twist. Fig. 5 shows the torsional angle calculation concept from pulse time difference information.

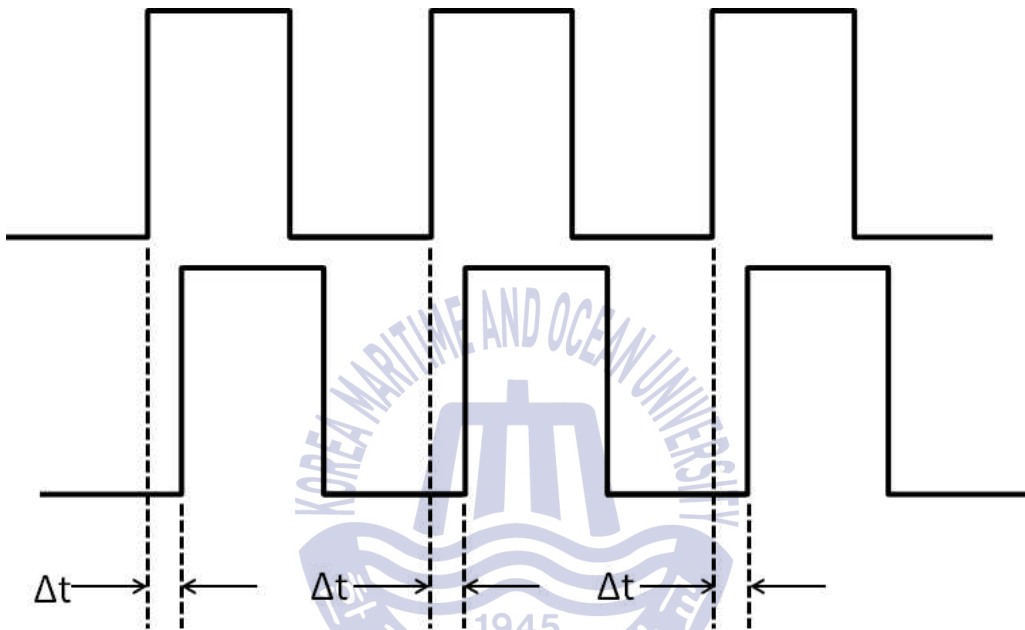


Fig. 5 Pulse difference in shaft rotation

As shown in Fig. 5, the time difference allows one to calculate torsional angle by using shaft diameter and shaft RPM.

Other than tachometer method there is also shaft vibration measurement system called vibrometer. A vibrometer works in a similar way as tachometer; however, it is highly advanced equipment that can measure various vibrations on a shaft. Similar to tachometer that calculates time difference to find torsional angle, a vibrometer also uses time difference to calculate torsional angle. The difference is that a vibrometer does not need a

piano tape, yet uses a proprietary reflective tape and has much higher accuracy than using tachometer. The two optical torque measuring systems are considered non-contact type torque sensors. The disadvantage of these non-contact torque sensors is that it needs two optical sensors to calculate torsional angle along with a computing unit. When torsional angle of a shaft is desired, one would need to setup two optical sensors (tachometer or vibrometer) then connect the sensors to the computing unit for data processing. Then the computing unit is once more connected to the user computer for data transfer. Optical non-contact type torque sensors are inconvenient to use due to many connections and multiple equipments. Also, the computing unit itself for vibrometer is very heavy to carry. However, non-contact type torque sensors are highly versatile than the contact type sensors due to the fact that it can measure various diameters of shafts. Both contact and non-contact torque sensors have limitations on measuring torque, yet non-contact type has more efficient measuring system.

Therefore, this paper introduces a new non-contact type torque measuring system to overcome the limitations of conventional non-contact type torque sensors using image technique torque measuring system.

3.2 Non-Contact Image Technique Based Torque Measurement

3.2.1 Experimental Setup

Torque measurement using image technique based on PIV (Adrian, 1991) is a new method and in order to test the accuracy of the technique a custom torque simulator had to be made. Fig. 6 is the basic layout of the torque simulator. The motor that drives the shaft is a DKM induction motor, and the model name of the motor is 9SDD2-60F2. The shaft that the motor is rotating was forged out of aluminum, and the following is the dimensions of the shaft: 40cm in length and 1.5cm in diameter. The imaging technique used in this paper uses high speed cameras and PIV to calculate torsional angle. High speed camera is chosen since ordinary smartphone cameras or DSLR cameras have limited shooting speed. Preferred high speed camera for this experiment is Phantom High speed camera. In order to successfully capture the torsional angle in the shaft, shooting speed of at least 1500 frames per second is needed. However, the shooting speed for this experiment is set to be 20,000 fps for increased accuracy. Also, to use PIV there must be random patterns for PIV program to recognize the angle displacement on the shaft. When random patterns are attached directly to the shaft, due to small diameter of the shaft, torsional angle is not very visible. Therefore, to maximize torsional angle visualization, two disks are added to either ends of the shaft. The added disks are also shown in Fig. 6 for reference. Then random patterns are attached on the edges of the disks. Since the patterns are attached at a further distance from the center of the shaft, the displacement of the patterns are more visible on the camera. Since there are two disks two high speed cameras are used for each disks with patterns.

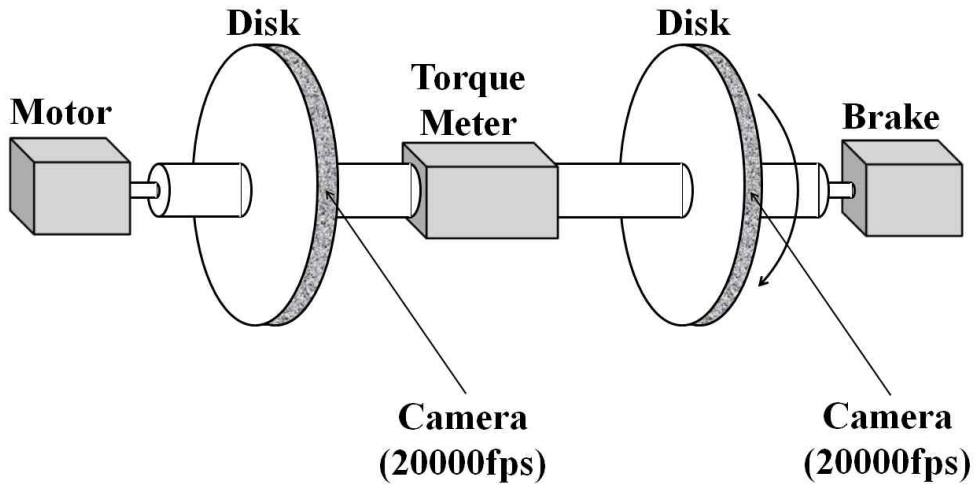


Fig. 6 Experimental Layout

In this experiment, it is important to synchronize the cameras to start shooting since slight delay of one camera would result in wrong torsional angle. Also, the motor used in this experiment must be very constant and reliable. When a motor is set to rotate at a certain RPM the motor is not actually rotating at that RPM. This is because the motor suffers from energy loss and needs to constantly apply current to achieve that RPM. When the rotation is too fast less current is applied and when rotation is too slow more current is applied. For example, a motor is set to rotate at 250 RPM. A motor with low current frequency the RPM variation would be ± 50 RPM. This is problematic because when RPM varies from 200 to 300 RPM, the torsional angle calculation becomes inconsistent. Therefore, to increase the accuracy of torsional angle a motor that is capable of supplying current with high frequency is highly suggested. In addition, it is important that the patterns attached to the shaft is random. The random pattern used in this experiment is shown in Fig. 7. The pattern is created by using black spray paint on a

paper. Since the patterns are sprayed, it creates great randomness to the patterns and is suitable for this experiment. There are several experimental errors one should watch out for that could cause substantial error in the outcome results.

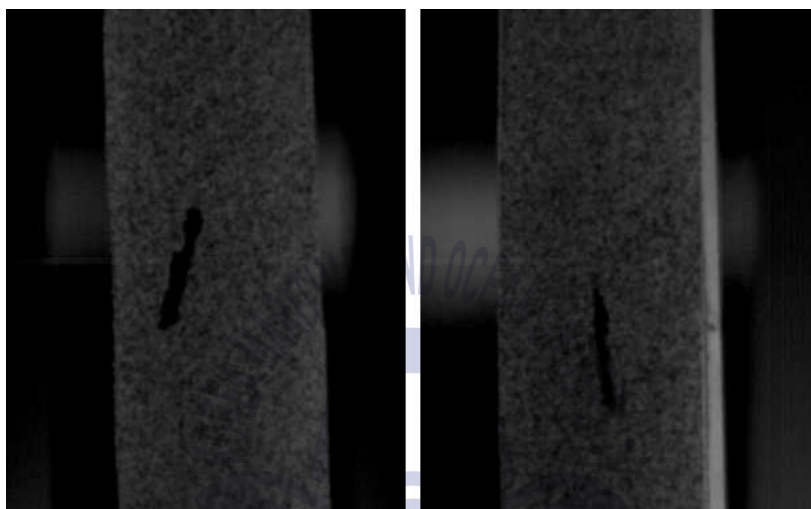


Fig. 7 Random Pattern (Left Image, Right Image)

First thing to notice is the exposure time of the camera. In this experiment, the exposure time is set to $1\mu s$ which is 0.000001 seconds. This is to minimize the pattern tearing as the RPM of the shaft increases. Fig. 8 and Fig. 9 shows images captured with different exposure times as RPM increases.

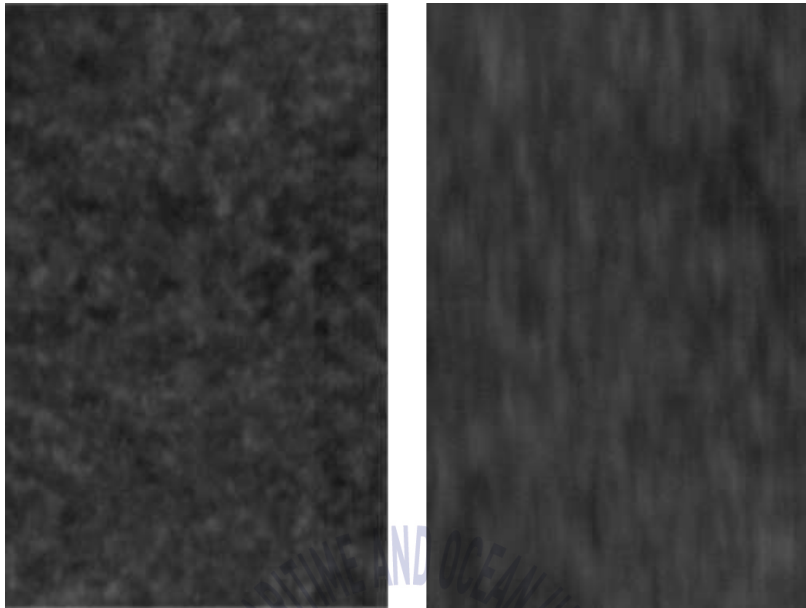


Fig. 8 Exposure time 0.000015s (Left 200 RPM, Right 1000RPM)

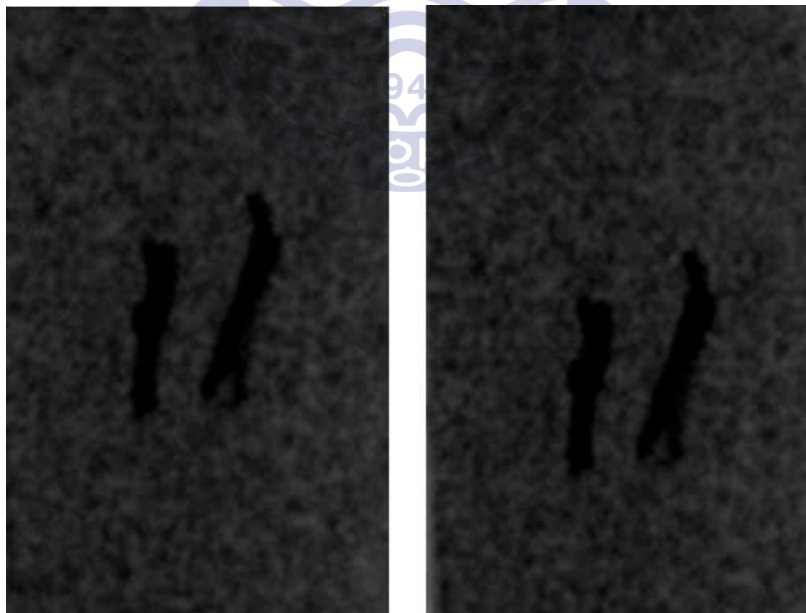


Fig. 9 Exposure time 0.000001s (Left 200 RPM, Right 1000RPM)

Fig. 8 shows images taken at 200RPM and 1000RPM with $15\mu s$ exposure time. Random pattern in 200RPM image is highly visible, yet random pattern in 1000RPM image is elongated. Since PIV method used in this study measures torsional angle by tracking random pattern, the outcome result may include error if the pattern is not very visible. Therefore, images in Fig. 8 are not suitable for image processing. The images shown in Fig. 9 are images with camera exposure time of $1\mu s$. Both, 200RPM image on the left and 1000RPM image on the right, show visible random pattern without elongated pattern. Thus, reducing exposure time as shown in Fig. 9 creates higher pattern visibility and is ideal for image processing.

Second thing to note is the lighting conditions of the surroundings. The lighting conditions are a crucial variable that must be considered when capturing high speed images. As previously mentioned, short exposure time is ideal for capturing visible random pattern; However, as exposure time becomes shorter, the light that the image sensor receives becomes less as well. Therefore, short exposure creates dark images. Dark images are not ideal for image processing since it hinders pattern visibility. In order to increase pattern visibility, it is highly recommended to perform the experiment in a brightly lit condition. Also, one must watch for what kind of light source is used for the experiment. If high speed images are captured using ordinary light source such as fluorescent light bulb, one may encounter a phenomena called flickering. Flickering is a subtle fading and increasing in luminosity of a light source. Most light source has this phenomenon and it is crucial to use a light source with minimum flickering effect. Since this experiment captures image with 20,000fps ordinary light bulbs with 60Hz of flickering is shown in the captured images. Flickering hinders the outcome of the calculated torsional angle due to inconsistent light intensity. Therefore, it is advised to use LED with DC power supply, LED with super high frequency, or tungsten

light bulb that has no frequency. In this experiment, multiple battery powered LED light sources were used.

Another source of error is material the pattern is drawn on to. When a bright light is applied to the pattern on the shaft, ordinary materials such as white paper reflects light. As shaft rotates the light reflection creates inconsistent light intensity. Inconsistent light intensity is not very ideal since it also creates error in the torsional angle calculations. Therefore, it is advised to use relatively unreflective materials such as kraft paper.

3.2.2 Experimental Procedure

Next is an experimental procedure for capturing the torsional angle of the shaft. The output rotation speed from the motor is given as 200, 300, 400, 500, 600, 700, and 800RPM. The torque is simulated twice with two different loads. Then the torsional angle calculated results using PIV method for each RPM cases are compared.

First, a stationary image of the pattern is captured and stored to memory cache. Then the shaft is rotated slowly to set angles to corresponding pattern. As a result, when the shaft rotates, the torsional angle can be calculated by the displacement difference between the fluctuating pattern and the position of the stored pattern. This is called calibration and one can start the experiment after calibration accurately set. Torque is then simulated by applying load to constant rotation speed of 200RPM. When the load is applied two synchronized high speed cameras captures the torsional angle between two positions. Then the captured images are stored for PIV calculation. After 200RPM is finished repeat the experiment for 300, 400, 500, 600, 700, and 800RPM respectively.

3.2.3 Image Technique Algorithm

The image technique used in this paper is Particle Image Velocimetry (PIV). There are multiple variations of PIV technique due to various possible applications. PIV can be categorized into two categories, high density PIV and low density PIV. Low density PIV is also referred as particle tracking velocimetry (PTV). In this paper PIV is utilized to capture the particle displacement.

PIV technique is useful when calculating displacement of particles in a given flow field or interrogation spot. Usually, in a flow field such as air, particles are so minuscule it is not very visible for human eyes or even cameras to see. Therefore, in order to capture and analyze the flow displacement of particles one injects particles into the flow field to visualize the flow movement. Then a camera projects the flow image for quantitative analysis. In this paper, in order to apply PIV technique, random pattern is applied to the shaft. Interrogation spot is then set at the random pattern to visualize the pattern movement.

As mentioned before, PIV is used to calculate the particle movement in an interrogation spot. This means that functions to quantify particle displacement is needed. A function that relates the particle movement in multiple images is called cross-correlation. Cross-correlation function correlates particle image pattern of continuously exposed images $f(x,y)$, and $g(x,y)$.

Let $p(x,y)$ to be a velocity vector point in a given interrogation spot. Then cross-correlation of two images $f(x,y)$, and $g(x,y)$ can be approximated by the following equation (2.14), convectonal integral.

$$CC_{fg}(\Delta X, \Delta Y) = \int_{-N}^N \int_{-N}^N f(X, Y)g(X + \Delta X, Y + \Delta Y)dx dy \quad (2.14)$$

Equation (2.14) illustrates the particle movement in x-direction and y-direction. However, cross-correlation method is sensitive to intensity changes of particle image pattern. Therefore, equation (2.14) is normalized to derive equation (2.15).

$$CC_{fg}(\Delta X, \Delta Y) = \frac{\sum_{i=-N}^N \sum_{j=-N}^N f(X_i, Y_j) - f_m g(X_i + \Delta X, Y_j + \Delta Y) - g_m}{\sqrt{\sum_{i=-N}^N \sum_{j=-N}^N f(X_i, Y_i) - f_m^2 \sum_{i=-N}^N \sum_{j=-N}^N g(X_i + \Delta X, Y_j + \Delta Y) - g_m^2}} \quad (2.15)$$

N in the equations (2.14) and (2.15) notes the number images.

Cross-correlation method alone is not enough to accurately calculate the particle movement since the particles may move within the pixel size. This means that the particle movement is smaller than a pixel, and particle movement in x and y-direction is not visible for cross-correlation method to calculate. In order to overcome this error, Cho (2004) introduced sub pixel interpolation, through which the location of correlation peak could be directly associated with particle displacements within the error of ± 0.5 pixels at the correlation peak locations. Several methods of interpolation have been introduced in the reference(Cho, 2004) in which the particle centroid have been calculated using the center of mass, the parabolic curve-fitting, and the Gaussian curve-fitting. Equations (2.16), (2.17), and (2.18) are for those methods, the center of mass, the parabolic, and the Gaussian methods, respectively.

$$P_{sub} = \frac{(i+1)R_{i+1} + iR_i + (i-1)R_{i-1}}{R_{i+1} + R_i + R_{i-1}} \quad (2.16)$$

$$P_{sub} = i - \frac{1}{2} \frac{R_{i+1} - R_{i-1}}{R_{i+1} - 2R_i + R_{i-1}} \quad (2.17)$$

$$P_{sub} = i - \frac{1}{2} \frac{\ln R_{i+1} - \ln R_{i-1}}{\ln R_{i+1} - 2\ln R_i + \ln R_{i-1}} \quad (2.18)$$

In this paper equation (2.18) is used for sub pixel interpolation since Gaussian method shows the best performance compared to other two methods (Scarano 2002). Fig. 10 shows the fractional error for each methods (Scarano 2002).

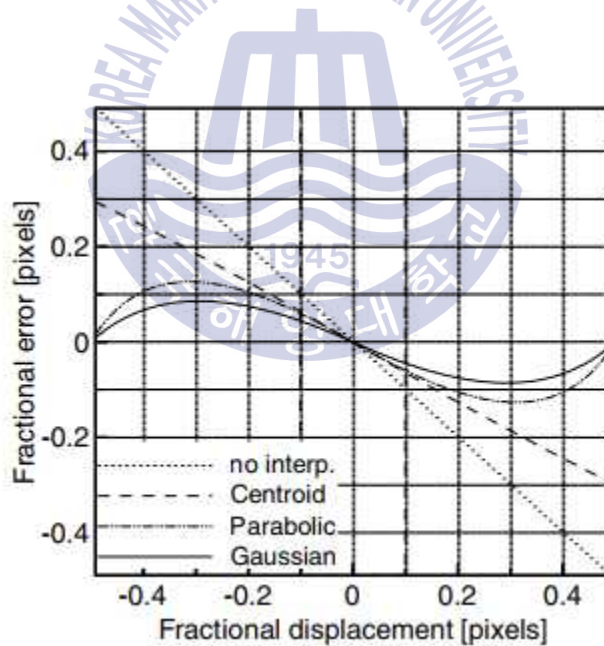


Fig. 10 Curve fitting error for common peak-fit functions

3.3 Experimental Results and Discussions

This Section contains the results of the experiment. First, the torque transducer measurement results are set as actual torque load on the shaft. The torque measurement through PIV is then compared to torque results from the torque transducer. Comparison results, discussions, and errors are listed in this section.

3.3.1 Torque Transducer Measurement Results

The results from torque transducer are illustrated in Table 1 and Table 2.

Table 1 Torque with respect to RPM, Load 1

RPM	200	300	400	500	600	700	800
Torque (kgf.cm)	4.41	4.57	4.81	4.92	5.10	5.53	5.66
Torque (Nmm)	432.47	448.16	471.70	482.49	500.14	542.31	555.06

Table 2 Torque with respect to RPM, Load 2

RPM	200	300	400	500	600	700	800
Torque (kgf.cm)	5.30	5.46	5.49	5.79	5.98	6.55	7.45
Torque (Nmm)	519.8	535.4	538.4	567.8	586.4	642.3	730.6

Table 1 and Table 2 each shows torque results for load 1 and load 2 at different RPM. Torque transducer outputs torque measurements in kgf.cm; however, kilogram force is not very intuitive for most people. Therefore, in the latter graphs torque units are labeled as Nmm. Fig. 11 and Fig. 12 shows

the torque results from torque transducer in graph format.

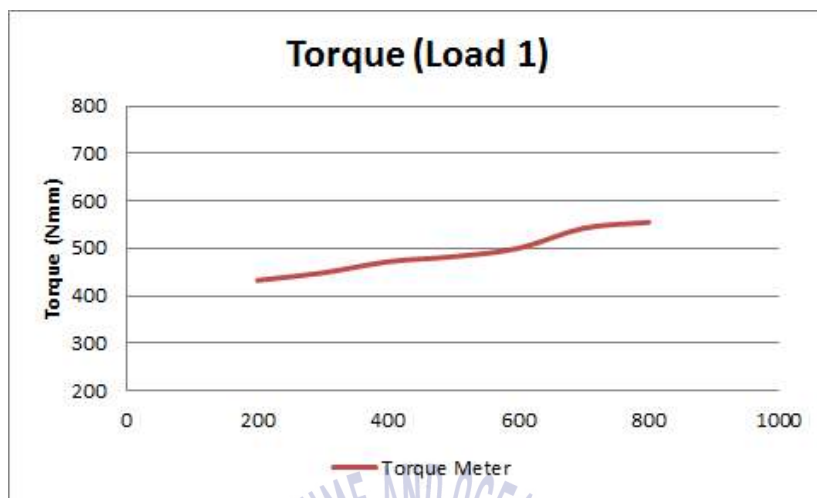


Fig. 11 Torque results from Torque Transducer for Load 1

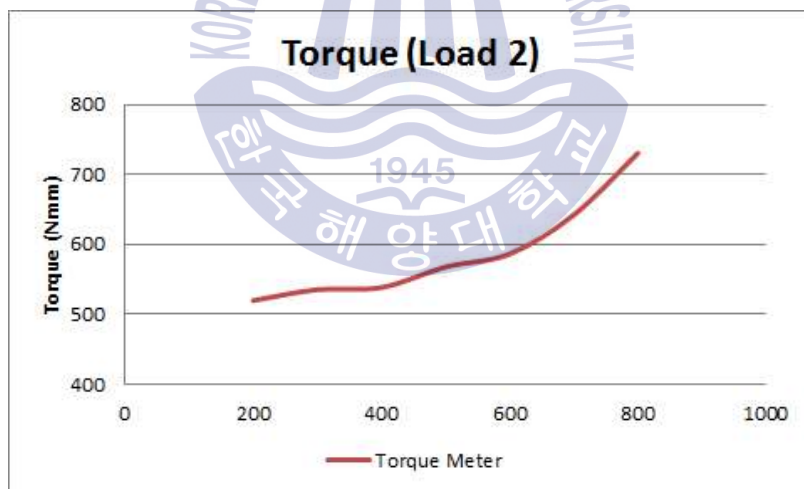


Fig. 12 Torque results from Torque Transducer for Load 2

From Fig. 11 and Fig. 12 one can notice that as RPM increases torque increases as well. Also, load 2 creates higher torque than load 1 since load 2 has higher load on the shaft than load 1.

3.3.2 PIV Based Torque Measurement Results

Fig. 13 and Fig. 14 shows angle change for 200RPM and 800RPM at load 2.

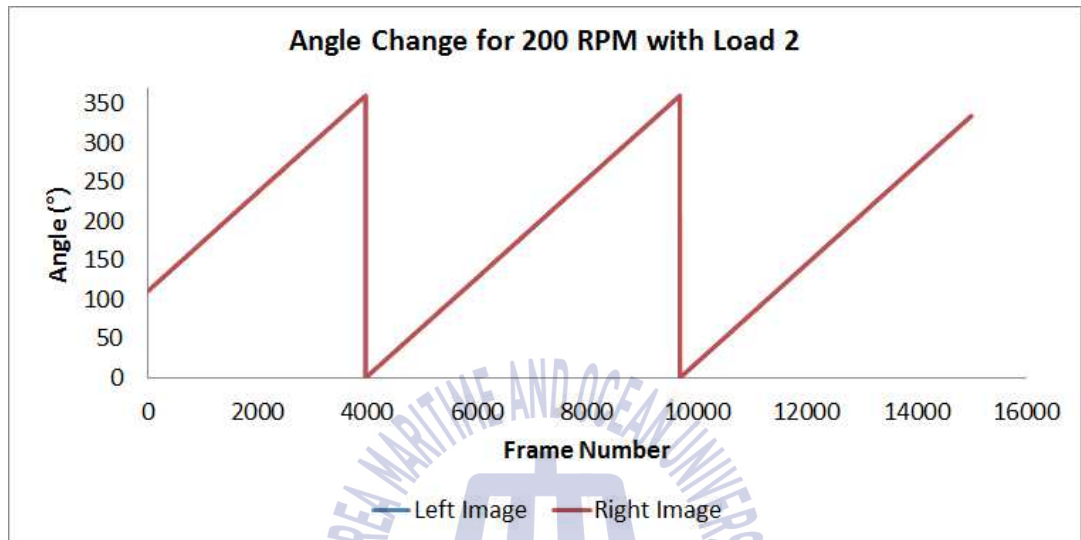


Fig. 13 Angle Change for 200 RPM with Load 2

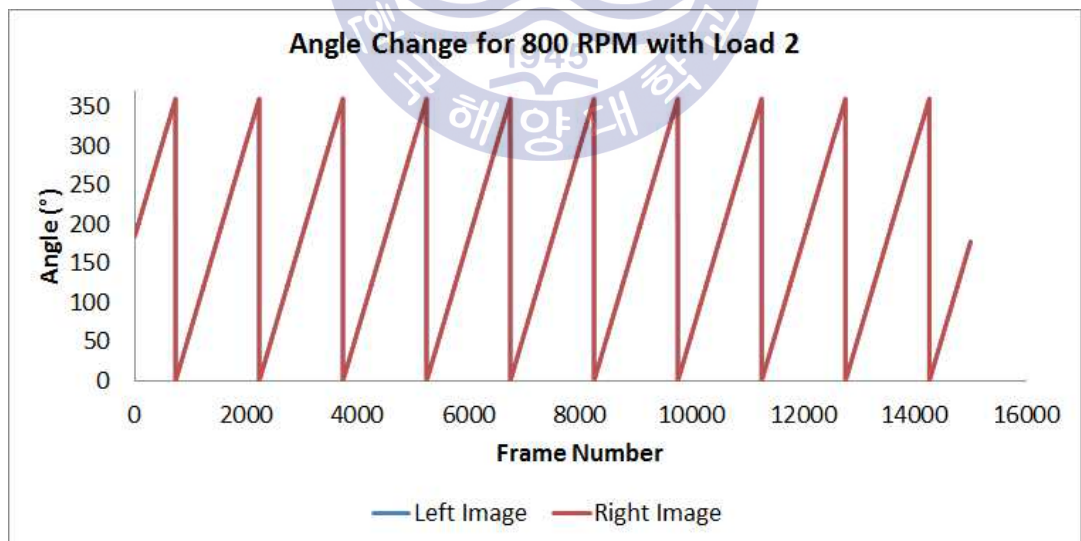


Fig. 14 Angle Change for 800 RPM with Load 2

It is evident that at same recording time, 800RPM rotates more than 200RPM due to higher rotating speed. Also, from Fig. 13 one can see that during the recording time the shaft rotated approximately 2.5 rotations. In Fig. 14 the shaft rotated approximately 10 rotations. At 200RPM 2.5 rotations were made, and at 800RPM 10 rotations were made. This shows that when RPM increased 4 times the rotations captured from camera also increased 4 times. The rotation ratio between two RPM shows that the recording was done correctly. Fig. 15 is a zoomed in version of Fig. 14 at its peak.

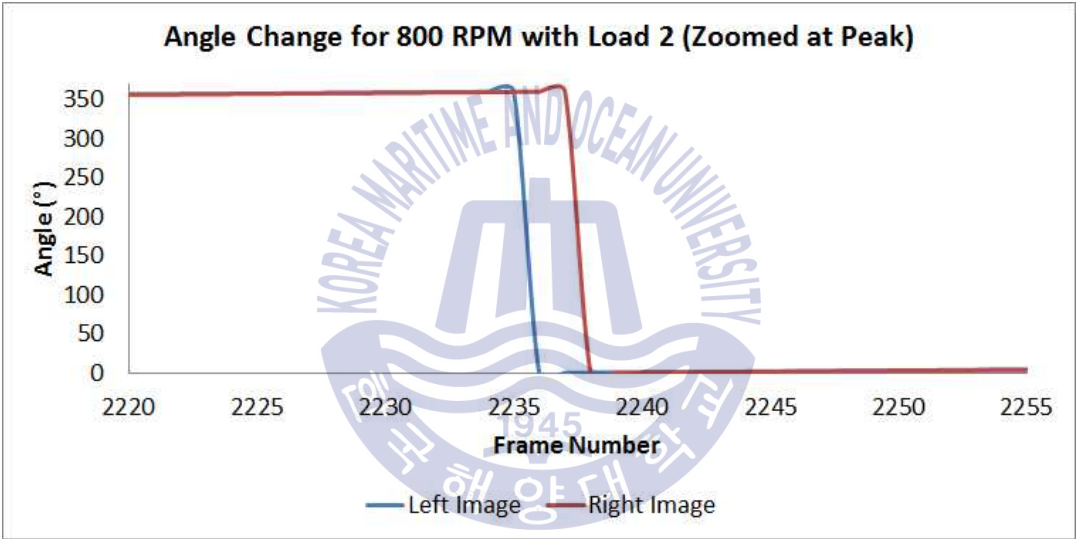


Fig. 15 Angle Change for 800 RPM with Load 2, Zoomed at peak

In Fig. 15, the left image (Blue line) completes one rotation then right image (Red line) completes one rotations afterwards. The meaning of this graph is very significant. The graphs shows that left part of the shaft is moving ahead the right part of the shaft. This means that the shaft is rotating with a twisted angle between two parts. Figures from Fig. 16 to Fig. 22 are graphical illustrations of torsional angles with load 1 acting on the shaft.

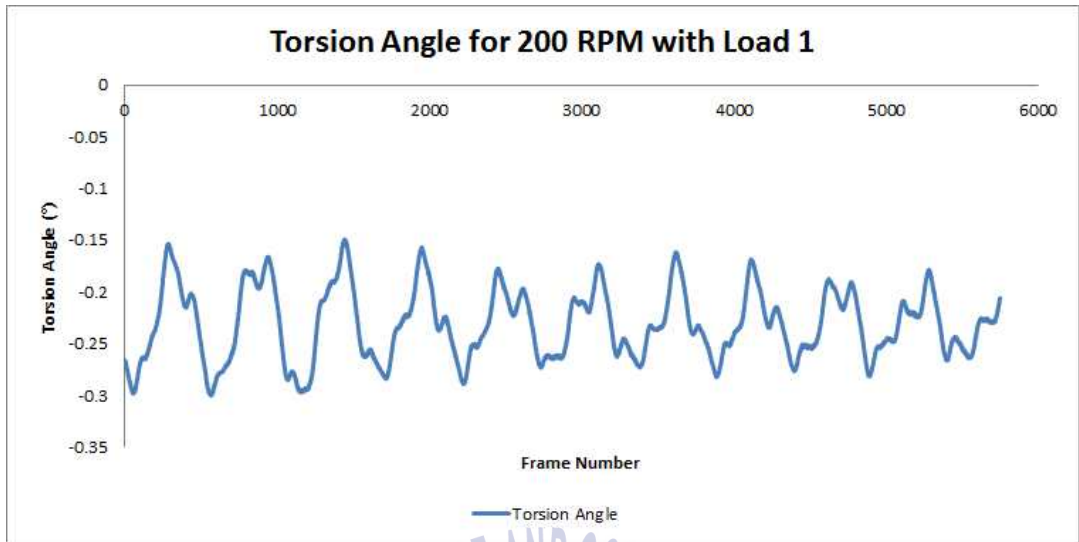


Fig. 16 Torsion Angle for 200 RPM with Load 1

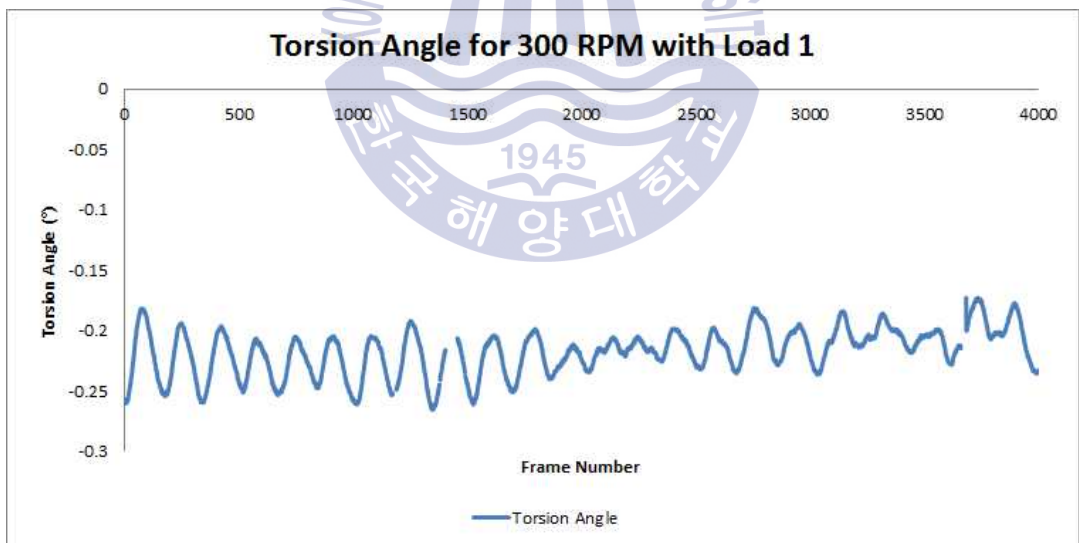


Fig. 17 Torsion Angle for 300 RPM with Load 1

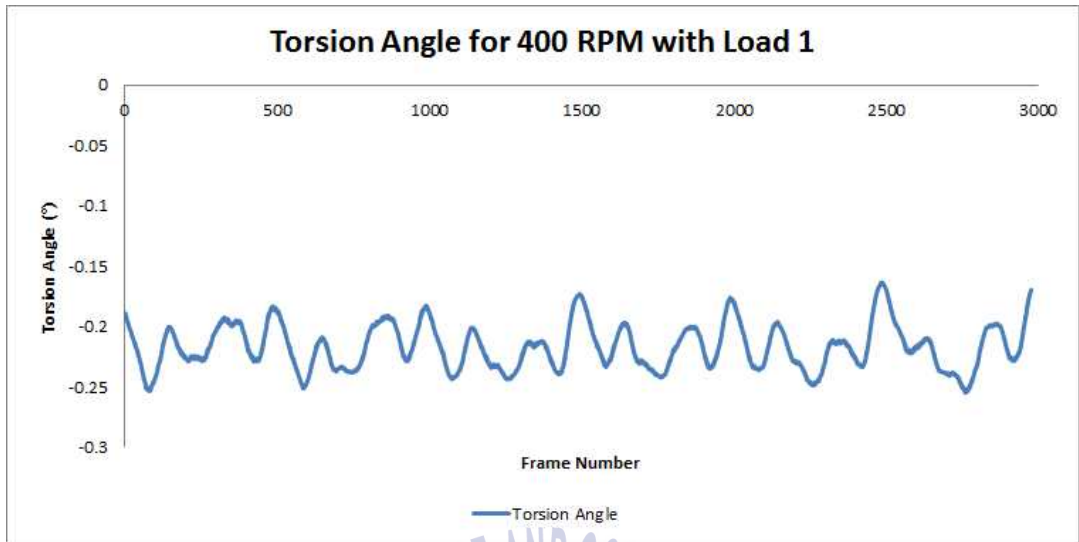


Fig. 18 Torsion Angle for 400 RPM with Load 1

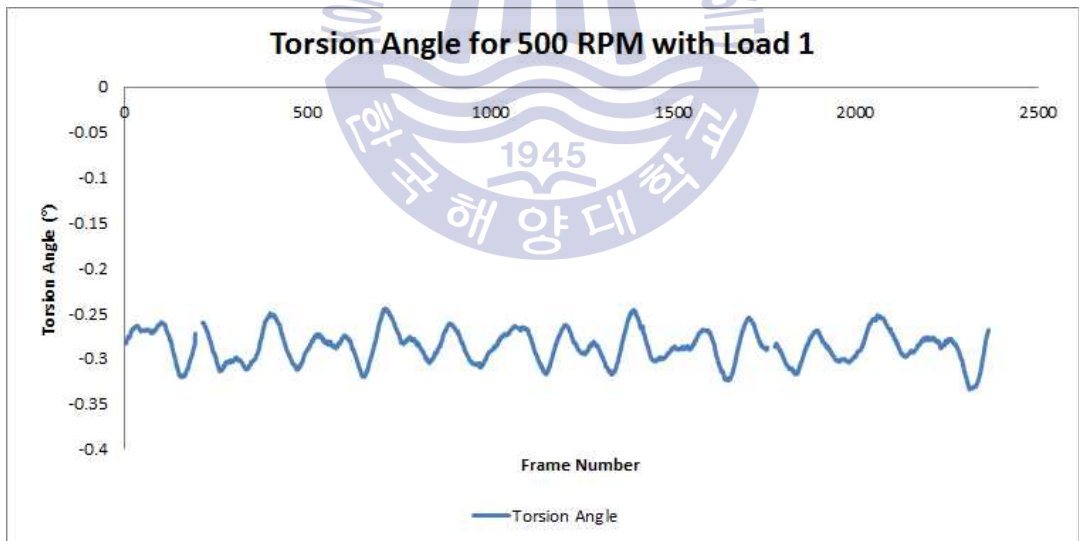


Fig. 19 Torsion Angle for 500 RPM with Load 1

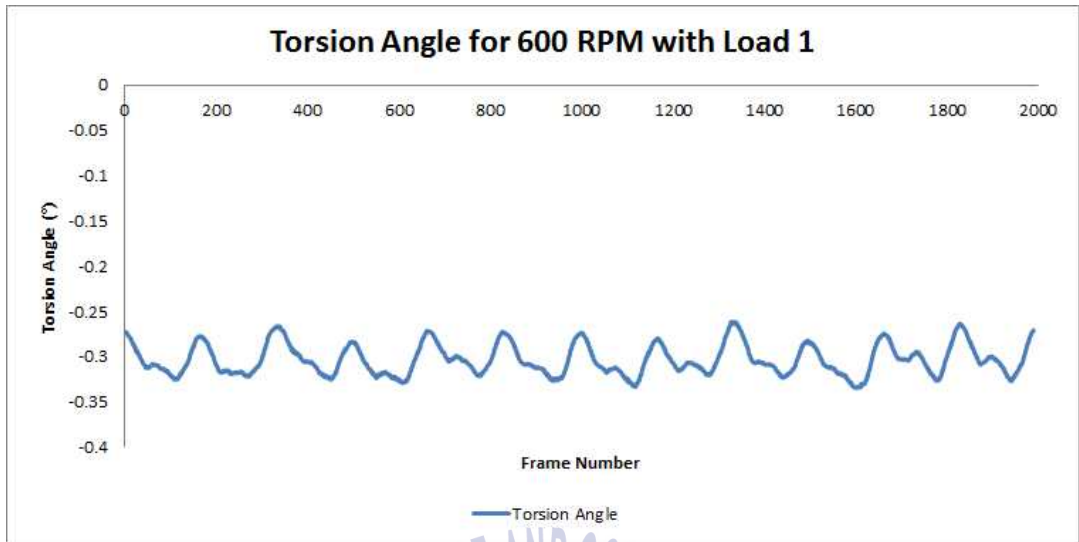


Fig. 20 Torsion Angle for 600 RPM with Load 1

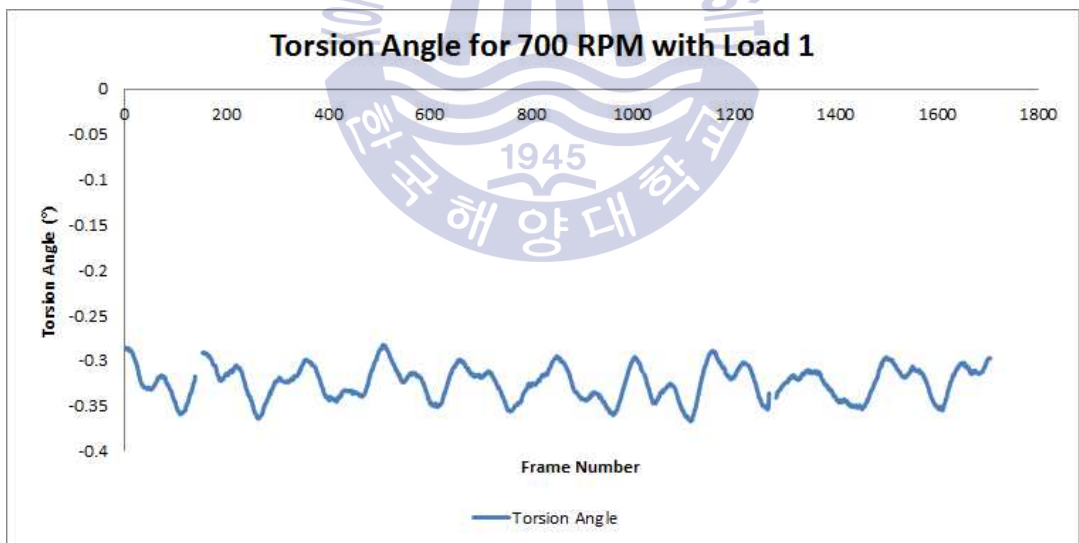


Fig. 21 Torsion Angle for 700 RPM with Load 1

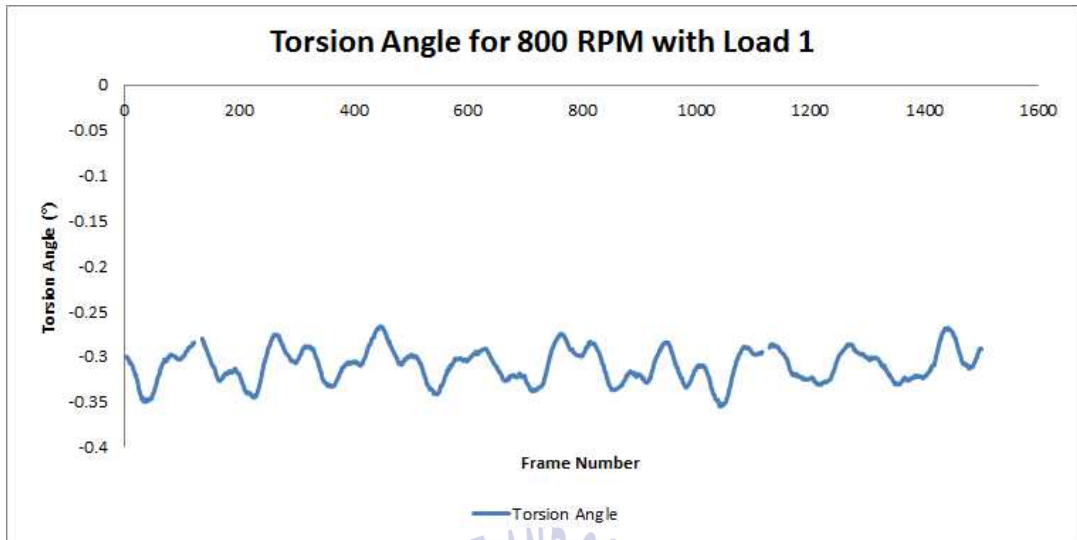


Fig. 22 Torsion Angle for 800 RPM with Load 1

Here, one can notice that torsional angle does not have linear relationship with RPM change. This is estimated that the coupling used in the torque simulator has non-linear properties and is affecting the torsional angle results. Also, empty spots can be seen in the figures. These empty spots are caused from small vibrations and dusts that disrupted the image during the recording; however, the empty spots are not significant to effect the outcome results. The torsional angle data was derived by taking average of the whole recorded torsional angles. Table 3 shows degree to radian conversion results.

Table 3 Torsion Angle with respect to RPM, Load 1

RPM	200	300	400	500	600	700	800
Degrees	-0.2311	-0.2170	-0.2170	-0.2863	-0.3032	-0.3242	-0.3095
Radians	-0.0040	-0.0038	-0.0038	-0.0050	-0.0053	-0.0057	-0.0054

Figures from Fig. 23 to Fig. 29 are graphical illustrations of torsional angles with load 2 acting on the shaft.

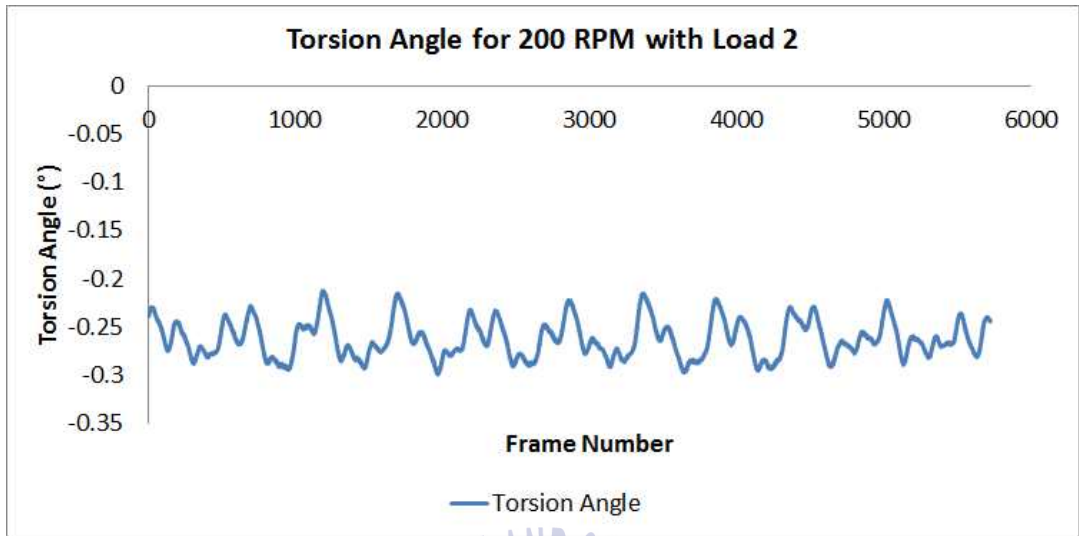


Fig. 23 Torsion Angle for 200 RPM with Load 2

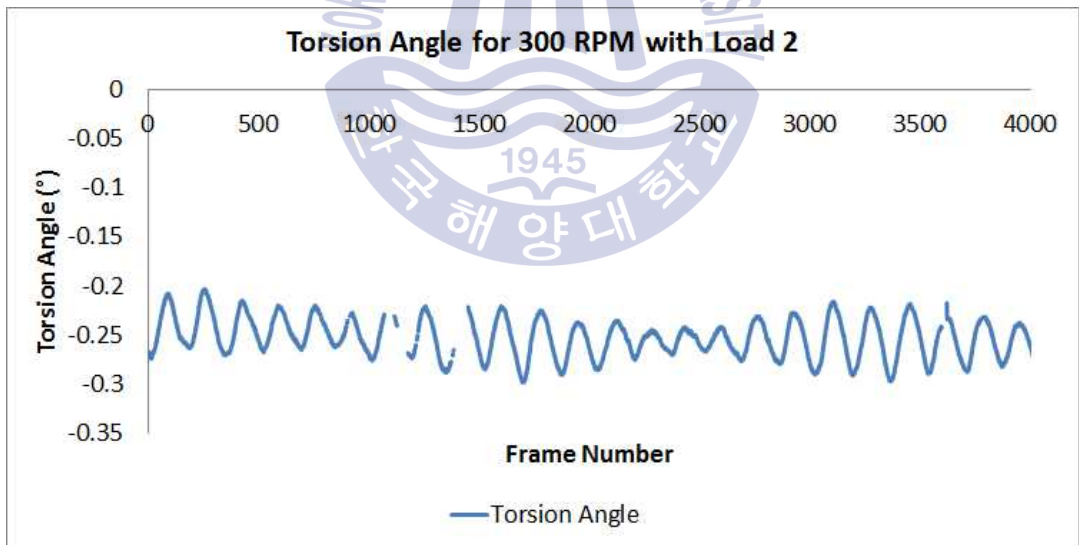


Fig. 24 Torsion Angle for 300 RPM with Load 2

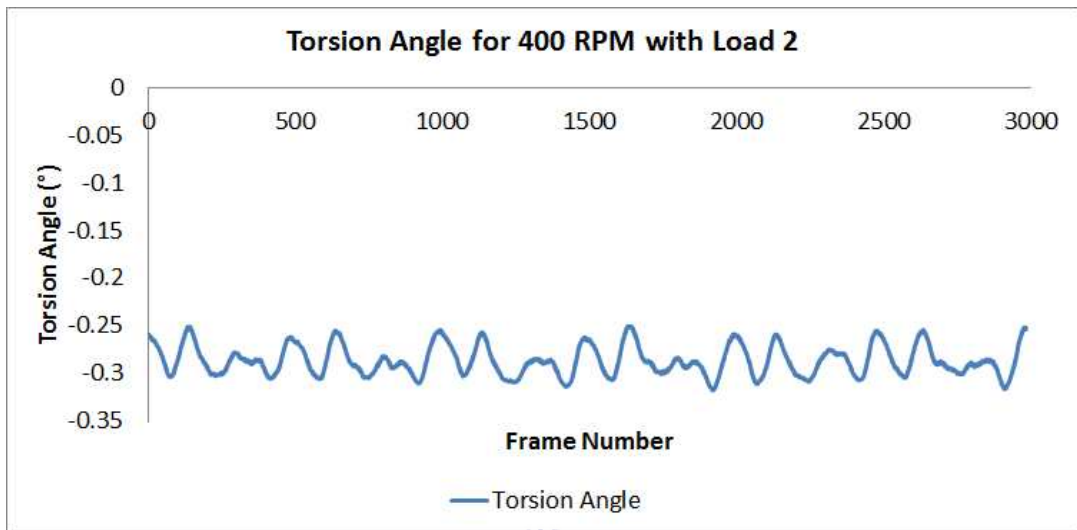


Fig. 25 Torsion Angle for 400 RPM with Load 2

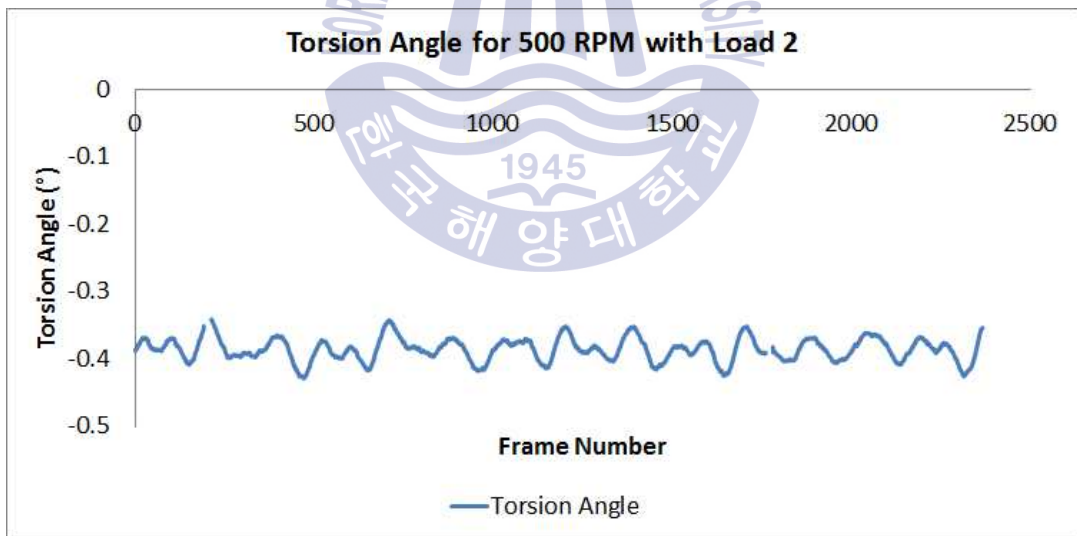


Fig. 26 Torsion Angle for 500 RPM with Load 2

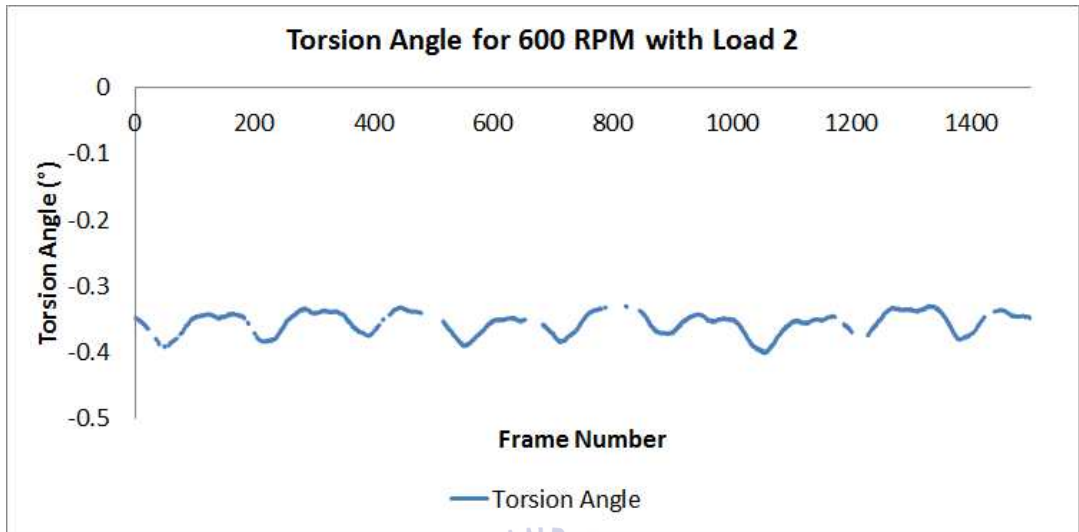


Fig. 27 Torsion Angle for 600 RPM with Load 2

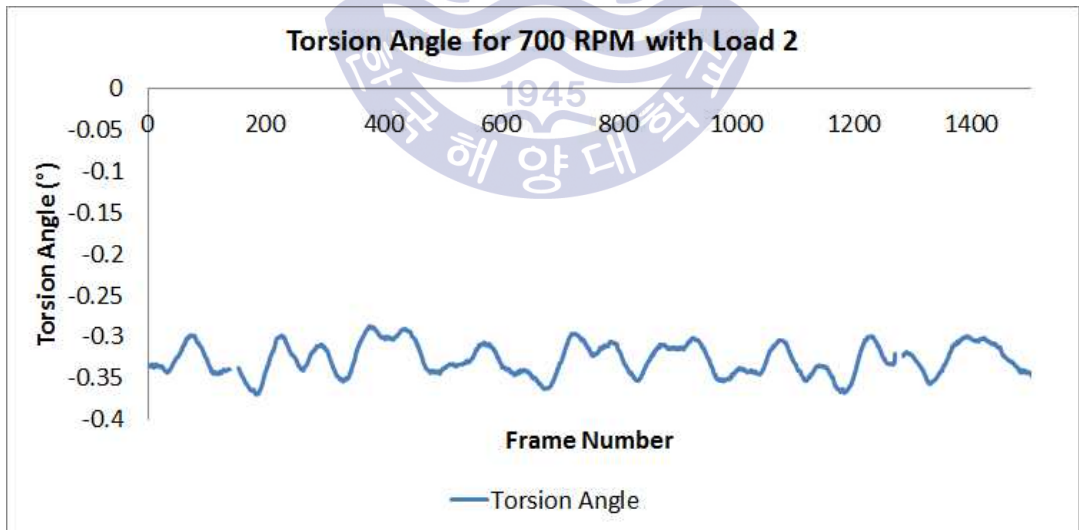


Fig. 28 Torsion Angle for 700 RPM with Load 2

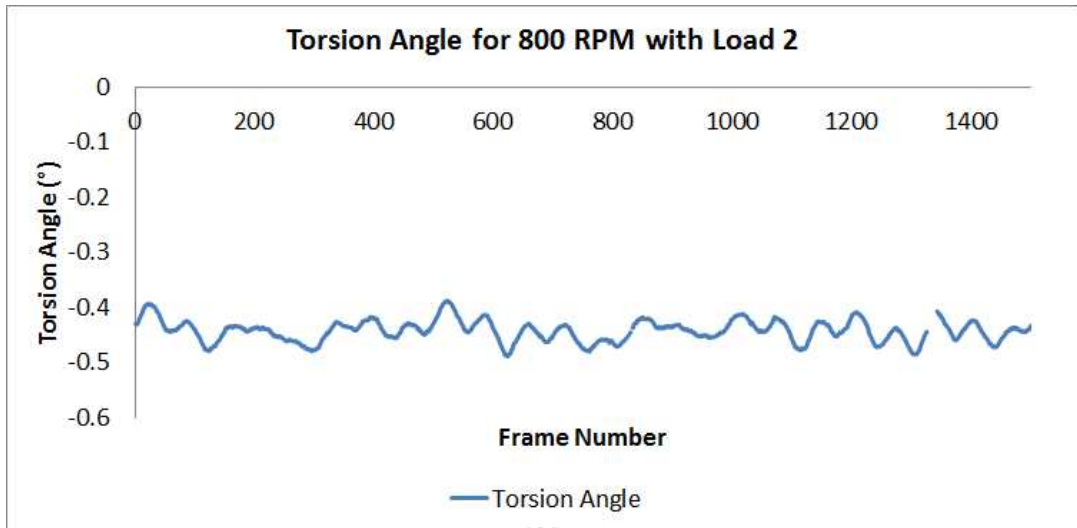


Fig. 29 Torsion Angle for 800 RPM with Load 2

Here also, one can notice that torsional angle does not have linear relationship with RPM change. This is estimated that the coupling used in the torque simulator has non-linear properties and is affecting the torsional angle results. Also, empty spots in the figures are caused from small vibrations and dusts that disrupted the image during the recording; however, the empty spots are not significant to effect the outcome results. The torsional angle data was derived by taking average of the whole recorded torsional angles. Table 4 shows degree to radian conversion results.

Table 4 Torsion Angle with respect to RPM, Load 2

RPM	200	300	400	500	600	700	800
Degrees	-0.2620	-0.2526	-0.2859	-0.3857	-0.3560	-0.3286	-0.4423
Radians	-0.0046	-0.0044	-0.0050	-0.0067	-0.0053	-0.0058	-0.0077

According to Table 3 and Table 4 it is evident that torsional angle does not have linear relationship with RPM speed. However, with different load at each RPM torsional angle increases linearly. This means that magnitude of torsional angle is non-linear with RPM speed, yet it is linear with load increase. Table 5 illustrates the linearity of torsional angle and load change.

Table 5 Torsion Angle with respect to RPM, Load 1 and Load 2

RPM	200	300	400	500	600	700	800
Load 1 (Radians)	-0.0040	-0.0038	-0.0038	-0.0050	-0.0053	-0.0057	-0.0054
Load 2 (Radians)	-0.0046	-0.0044	-0.0050	-0.0067	-0.0062	-0.0058	-0.0077

Now that torsional angle is derived from experiment, one can calculate torque applied to the shaft. According to equation (2.12) torque can be calculated by multiplying torsional angle and torsional stiffness. Since torsional angle is derived through experiment, torsional stiffness is the only unknown variable.

Torsional stiffness of the shaft can be calculated through equation (2.11). According to equation (2.11) to find torsional stiffness k , shaft length L , shear modulus of the shaft G , and 2nd moment of inertia J variables are needed. The length of the shaft is 400mm. Since the material of the shaft is made out of aluminum the shear modulus is 77.2GPa or 772010MPa. The only unknown variable is J . The equation (2.19) is the equation to calculate 2nd moment of inertia.

$$J = \frac{\pi d^4}{32} \quad (2.19)$$

Here,

d : diameter of the shaft (mm)

The diameter of the shaft is approximately 1.5cm or 15mm. By substituting diameter to equation (2.19), the result of 2nd moment of inertia becomes 4970.1mm⁴. Since all the unknown variables L , G , and J are found, one can calculate torsional stiffness by using the equation (2.11). Substituting the variable to equation (2.11), the torsional stiffness is calculated to be 959229.3Nmm/rad.

The equation to calculate torque is shown in equation (2.12). By substituting torsional angle and torsional stiffness to the equation one can successfully calculate torque. Table 6 show the calculated torque for each RPM with load 1 and load 2.

Table 6 Torque with respect to RPM

RPM	200	300	400	500	600	700	800
Torque (Load 1)	3836.9 Nmm	3645.1 Nmm	3645.1 Nmm	4796.2 Nmm	5083.9 Nmm	5467.6 Nmm	5179.8 Nmm
Torque (Load 2)	4412.5 Nmm	4220.6 Nmm	4796.2 Nmm	6426.8 Nmm	5947.2 Nmm	5563.5 Nmm	7386.1 Nmm

The results in Table 6 are calculated by multiplying torsional angle to torsional stiffness. One must note that the torsional stiffness calculated previously had negative values. This is because the direction of the twist accounts for the negative or positive signs. Therefore, the negative sign can be neglected. Fig. 30 and Fig. 31 are graphical representations of the results in Table 6.

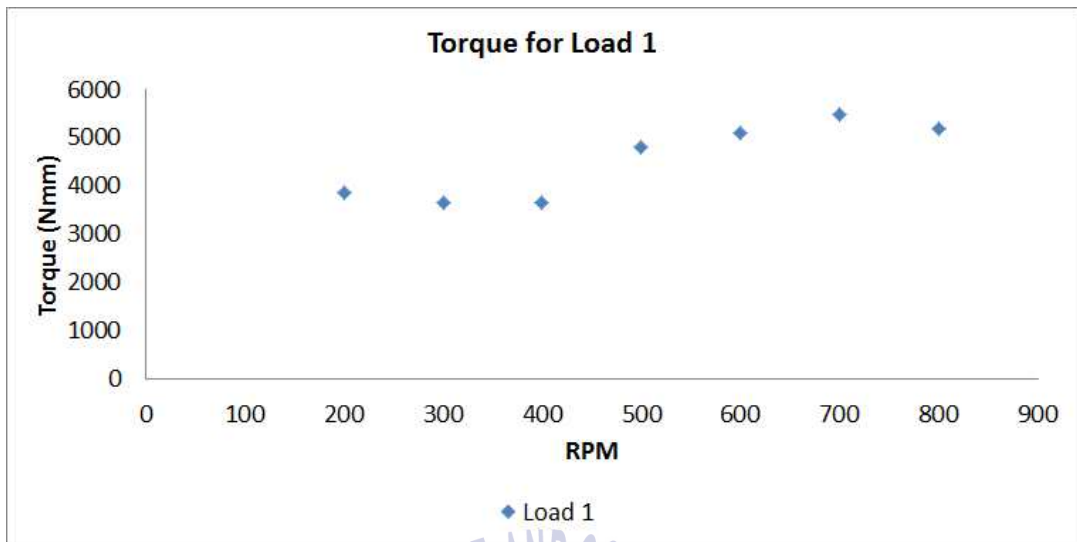


Fig. 30 Torque for Load 1

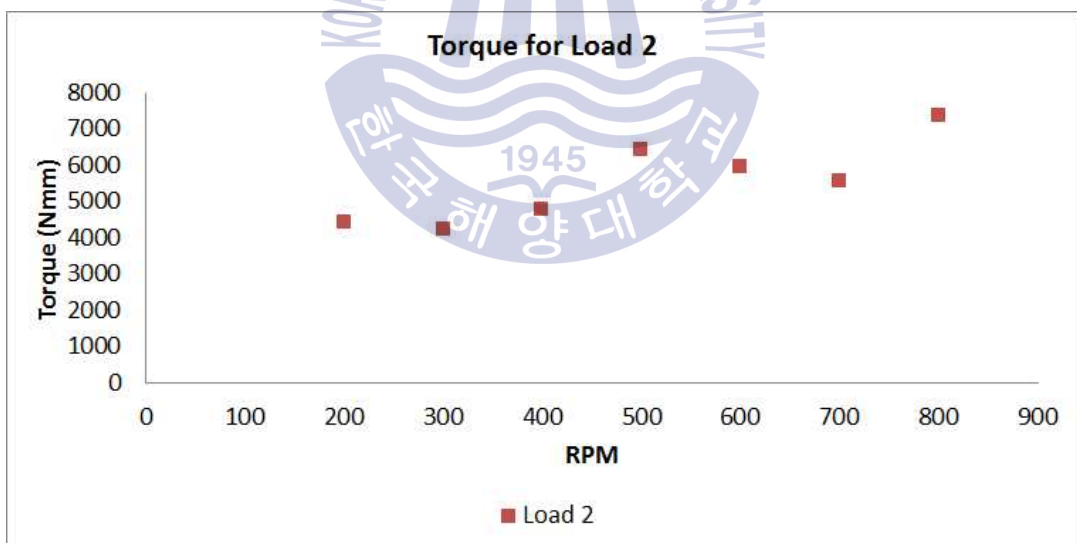


Fig. 31 Torque for Load 2

Overall, magnitude of torque in Fig. 30 is smaller than magnitude of torque in Fig. 31. This result is natural since shaft in Fig. 30 has less load than shaft on Fig. 31.

3.3.3 Measurement Results Comparison

Comparing torque results from Table 1 and Table 2 to Table 6 shows large magnitude difference. Table 7 and Table 8 shows the error ratio of torque transducer results and PIV torque measurement results.

Table 7 Torque value ratio for Load 1

RPM	200	300	400	500	600	700	800
Torque- Transducer (Nmm)	432.47	448.16	471.70	482.49	500.14	542.31	555.06
PIV Method (Nmm)	3836.9	3645.1	3645.1	4796.2	5083.9	5467.6	5179.8
Ratio	8.87	8.13	7.73	9.94	10.16	10.08	9.33

Table 8 Torque value ratio for Load 2

RPM	200	300	400	500	600	700	800
Torque- Transducer (Nmm)	519.8	535.4	538.4	567.8	586.4	642.3	730.6
PIV Method (Nmm)	4412.5	4220.6	4796.2	6426.8	5947.2	5563.5	7386.1
Ratio	8.49	7.88	8.91	11.32	10.14	8.66	10.11

According to Table 7 and Table 8, in both load 1 and load 2 cases, the torque results vary from 7 times to 10 times. The visualization of the error is illustrated in Fig. 32 and Fig. 33.

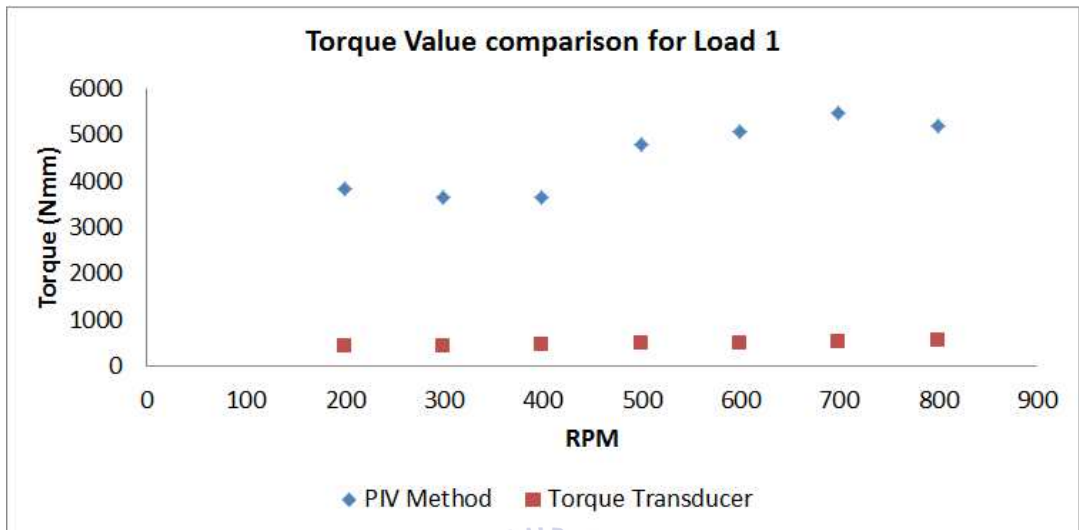


Fig. 32 Torque value comparison for Load 1

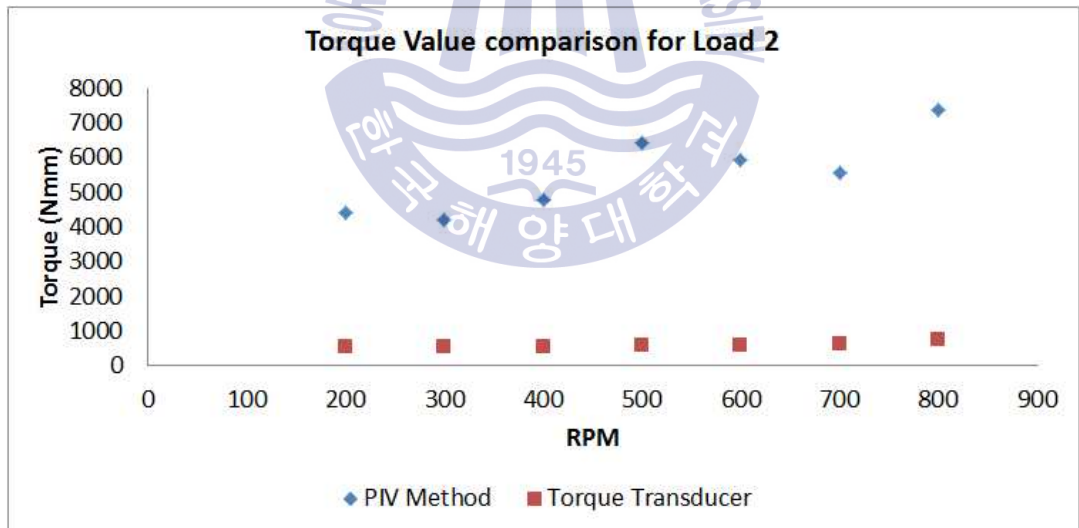


Fig. 33 Torque value comparison for Load 2

The reason for the large error in the torque magnitude is that only the torsional stiffness of the shaft is considered, and torsional stiffness of the couplings in the shaft are omitted. Most shafts that are connected to engines of gears have couplings, and these couplings also have torsional stiffness that account for the torsional angle in the shaft. The shaft used in this experiment also has two couplings that connect motor to the shaft, and the torsional stiffness of the two couplings also must be considered for accurate torque measurement.

3.3.4 Relevance of Coupling Stiffness

According to product catalogue of Highly flexible GKN STROMAG PERIFLEX VN DISC COUPLING from Stromag (2016), Stromag recommends that when calculating torque with coupling attached to the shaft multiply 0.7 and 1.35 to the coupling torsional stiffness. This is to compensate for the non-linear torsional stiffness behaviour of couplings. The torsional stiffness of a coupling changes when the coupling heats up. Also, when the RPM is low and the load on the coupling is weak the torsional stiffness of the coupling changes. Therefore, to compensate for both cases Stromag recommends to multiply 0.7 and 1.35 to the torsional stiffness of the attached coupling.

Also, another coupling company Vulkan also sets a similar standard to calculate torsional stiffness. According to EXPLANATION OF TECHNICAL DATA from Vulkan Couplings (2016), it states that in case of low twist amplitude the torsional stiffness is “equivalent to $1.35 C_{Tdyn}$ ”. Also, Vulkan Coupling (2016) states that when temperature is considered the torsional stiffness is “equivalent to $0.7C_{Tdyn}$ ”. Therefore, it is important to consider torsional stiffness of the couplings to accurately calculate torque in the shaft.

3.3.5 Revised Torsional Stiffness Results

Fig. 34 and Fig. 35 shows the torque results after including coupling torsional stiffness.

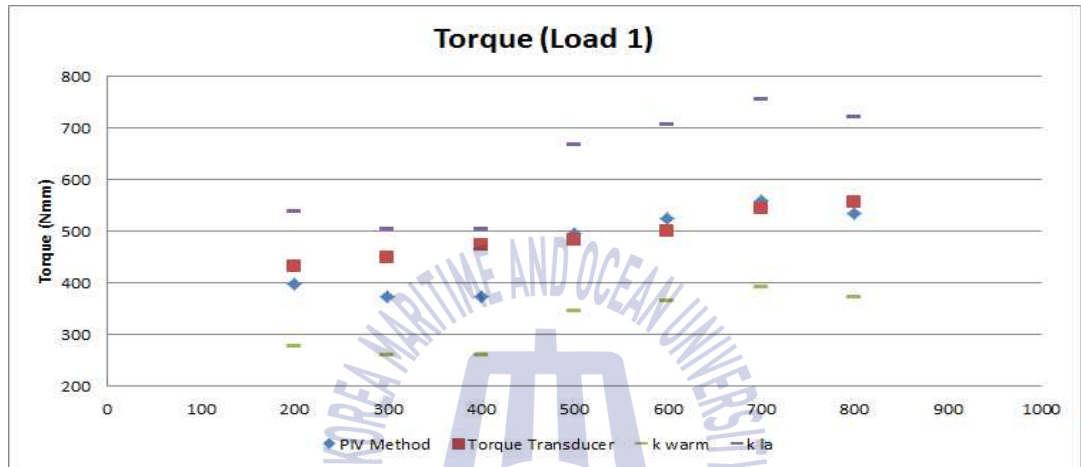


Fig. 34 Torque value comparison for Load 1 (Coupling added)

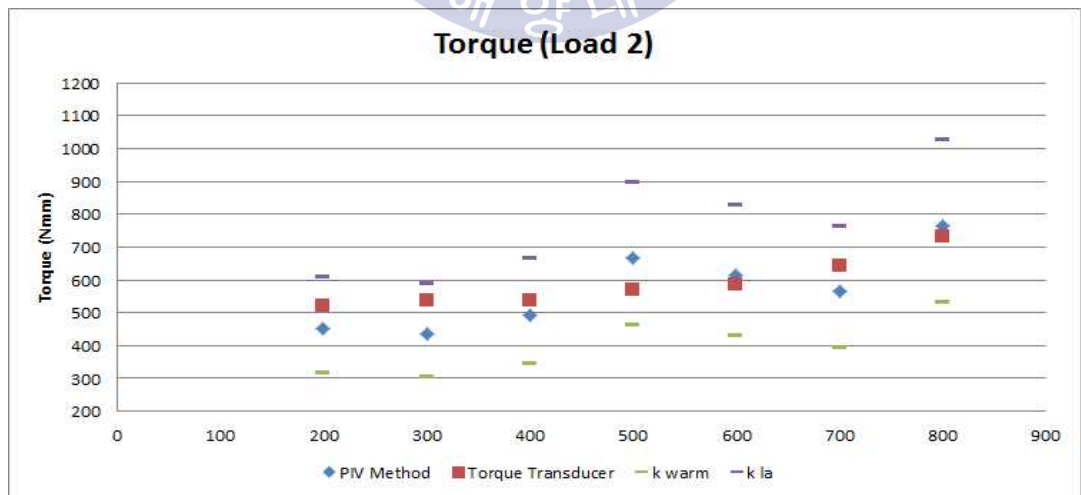


Fig. 35 Torque value comparison for Load 2 (Coupling added)

From Fig. 34 and Fig. 35 one can see that after applying coupling torsional stiffness, the torque error between PIV method and torque transducer have reduced significantly. Also, all the torque measurement values are within the boundary of 0.7 and 1.35 stiffness range. Table 9 and Table 10 illustrates the torque magnitude ratio of the two methods.

Table 9 Torque value ratio for Load 1 (Coupling added)

RPM	200	300	400	500	600	700	800
Torque- Transducer (Nmm)	432.47	448.16	471.70	482.49	500.14	542.31	555.06
PIV Method (Nmm)	395.57	374.16	374.17	493.69	523.02	559.11	533.81
Ratio	0.91	0.83	0.79	1.02	1.05	1.03	0.96

Table 10 Torque value ratio for Load 2 (Coupling added)

RPM	200	300	400	500	600	700	800
Torque- Transducer (Nmm)	519.8	535.4	538.4	567.8	586.4	642.3	730.6
PIV Method (Nmm)	451.82	435.58	493.12	665.21	613.95	566.68	762.84
Ratio	0.87	0.81	0.92	1.17	1.05	0.88	1.04

Table 9 and Table 10 illustrates the accuracy of the PIV method compared to torque transducer. For load 1 the minimum accuracy is 79% and maximum accuracy is 102%. For load 2 the minimum accuracy is 81% and maximum accuracy is 104%.

3.3.6 Power Results

Using the calculated results from previous parts, power applied to the shaft can also be calculated. Table 11 and Table 12 shows the calculated power for load 1 and load 2.

Table 11 Power value for Load 1

RPM	200	300	400	500	600	700	800
Torque- Transducer (W)	8.35	11.75	15.67	25.85	32.86	40.99	44.72
PIV Method (W)	9.24	14.36	20.13	25.76	32.04	40.54	47.42

Table 12 Power value for Load 2

RPM	200	300	400	500	600	700	800
Torque- Transducer (W)	9.46	13.68	20.66	34.83	38.58	41.54	63.91
PIV Method (W)	11.09	17.15	23.00	30.32	37.59	48.01	62.41

Fig. 36 and Fig. 37 are graphical representations of Table 11 and Table 12.

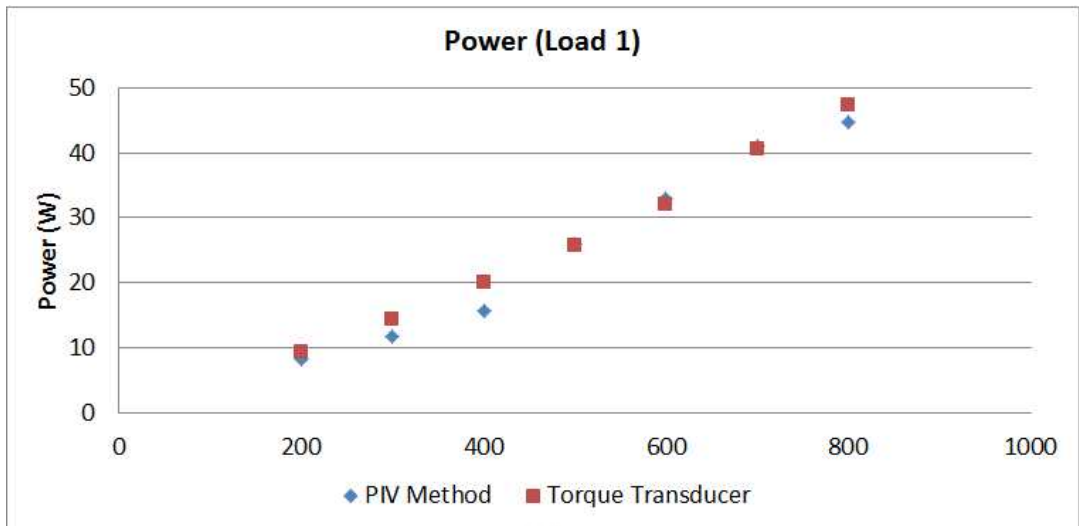


Fig. 36 Power value comparison for Load 1

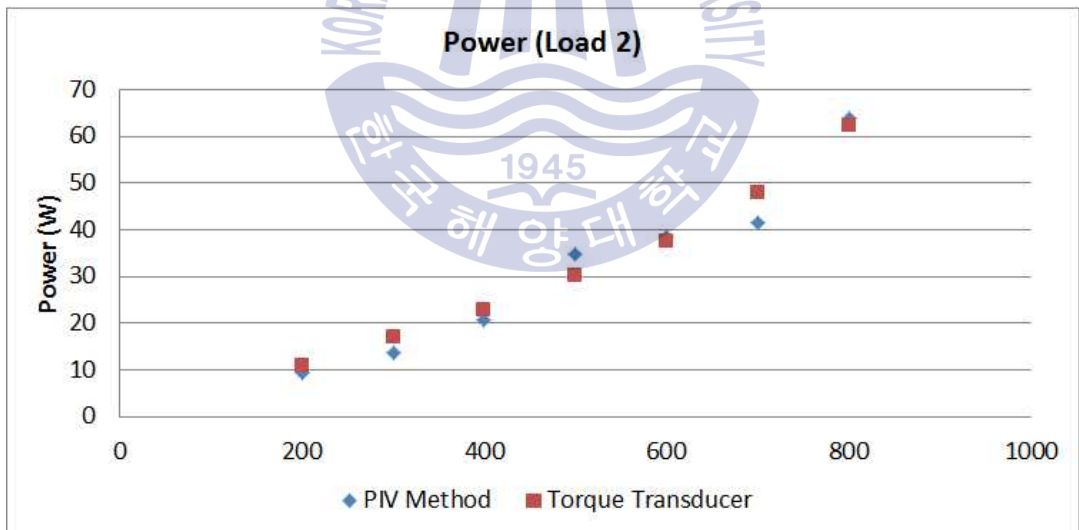


Fig. 37 Power value comparison for Load 2

4. Conclusion

Conventional torque measuring methods such as using Shaft Power meter or vibrometer are very expensive and inconvenient to use.

This paper successfully introduces a new way of measuring torque using imaging technique. The utilized image technique is based on Particle Image Velocimetry (PIV). By using PIV the torsional angle constructed by the load on the shaft was obtainable with high precision.

Through obtained torsional angle, torque was calculated and the resulting torque values were then compared to the torque results obtained from torque transducer. Torque transducer is a contact type torque measuring device that accurately measures torque on a loaded shaft. The comparison of the two methods would prove the accuracy and precision of PIV torque measuring technique.

At a weak load (load1) the average accuracy of PIV method was calculated to be 94% with minimum accuracy of 79%. At strong load (load 2) the average accuracy of PIV method was calculated to be 96% with minimum accuracy of 81%. From these results, it can be concluded that torque measuring technique using PIV is highly promising for predicting the power of the rotational shaft with further improvement, revealing possible replacement of conventional torque measuring sensors.

Reference

- Adrian, R.J., 1991. Particle-Imaging Techniques for Experimental Fluid Mechanics. *Annual Review of Fluid Mechanics*, 23, pp.261-304.
- Cho, G.R., 2004. *Improvement of Stereoscopic PIV and its application on the two types of impeller of multi-blade fan*. Ph.D. Saitama: Saitama University, pp.11-15.
- Jeon, M.G. Cho, G.R. Lee, K.K. & Doh, D.H., 2015, A Monitoring System Based on an Artificial Neural Network for Real-Time Diagnosis on Operating Status of Piping System, *KSME(B)*, 39(2), pp.199-206.
- Kyma, 2010. *Kyma Shaft Power Meter Continuous measurement of torque, power and revolutions*, Bergen: Kyma.
- Polytech, 2017. *IVS-500 Industrial Vibration Sensor Acoustic Quality Control with Laser Precision Product Brochure*, Waldbronn: Polytech.
- Scarano, F., 2002. Iterative image deformation methods in PIV. *Institute of Physics Publishing Meas. Sci. Technol.* 13, pp.R1-R19.
- Stromag, 2014. *Highly flexible GKN STROMAG PERFLEX VN DISC COUPLING*, Unna: Stromag.
- Vulkan Couplings, 2016. *EXPLANATION OF TECHNICAL DATA*, Herne: Vulkan Group, pp.19.

감사의 글

본 논문이 완성될 때까지 석사과정에서 대학원 과정을 지도하여 주신 한국해양대학교 냉동공조공학과와 기계공학의 모든 교수님께 감사드리며, 특히 논문 완성에 있어 세심한 배려와 지도를 아끼지 않으신 도덕희 교수님께 감사를 드립니다. 언제나 학생들을 위해 고민하시고 일하시는 교수님의 모습은 부족한 저에게 많은 것을 느끼고 배울 수 있도록 해주셨습니다. 그리고 바쁜 와중에도 논문을 완성하는데 도움을 주신 김동혁 교수님, 김성춘 박사님께 감사의 말씀을 전합니다.

논문의 실험 결과에 문제점과 개선방안 등 많은 도움을 주신 조경래 박사님, 진동 개요와 진동의 전반적인 지식을 전수해 주신 김의간 교수님과 김형진 선배님, 밤늦게도 실험에 많은 도움을 주었던 동익 형이랑 대경이, 연구와 공부에 도움이 되는 교육 참석을 권해준 준호 형, 그리고 언제나 실험실에서 밝게 맞이해주었던 경원이 형이랑 산이 그리고 성진이를 비롯한 모든 실험실 식구에게도 감사의 말을 전하고 싶습니다.

항상 집과 교회를 오가시며 논문 완성을 위해 기도해주신 어머니와 보이지 않는 곳에서 많은 도움을 주신 아버지 그리고 나를 위해 응원해준 가족에게도 감사의 말씀을 전합니다.

주변의 모든 분들이 도움을 주지 않았다면 이 논문이 완성되기 힘들었을 것이라고 믿습니다. 긴 기간 동안 옆에서 응원해주신 모든 분들께 머리 숙여 깊이 감사드립니다. 감사합니다.

2018년 1월

김영환 올림